

PROBING QUANTUM CAPACITANCE OF 2D MATERIALS USING NOVEL TECHNIQUE

BY AKSHAY RANCHHOD PATIL
Advisor – Prof. Chandni Usha



CONTENTS

- MOTIVATION
- QUANTUM CAPACITANCE
- TECHNIQUES OF MEASURING QUANTUM CAPACITANCE OF 2D MATERIALS
- EXPERIMENTAL PROCEDURES INVOLVED
- EXTRACTION OF PHYSICAL QUANTITIES FROM QUANTUM CAPACITANCE.
- FUTURE SCOPE/OUTLOOKS/IMPACTS OF THIS WORK IN QUANTUM TECHNOLOGIES
- CONCLUSION
- REFERENCES

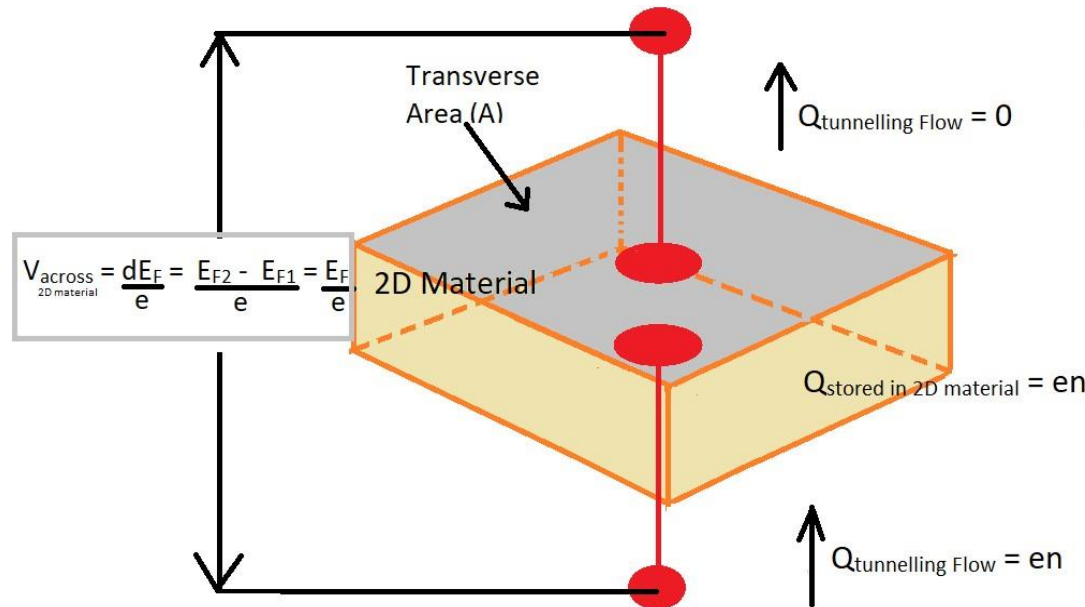


MOTIVATION FOR PROBING Q.C OF 2D MATERIALS

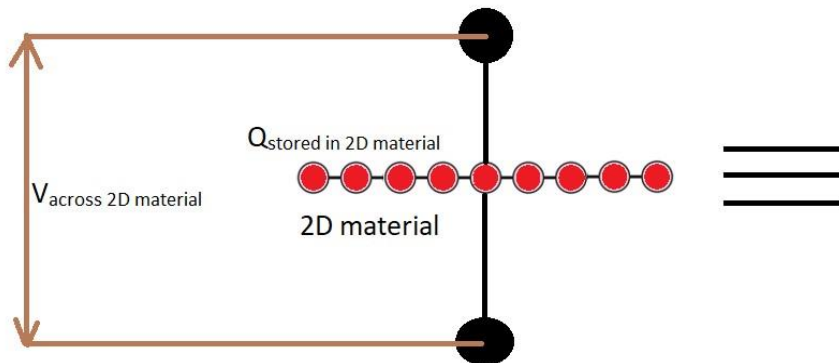
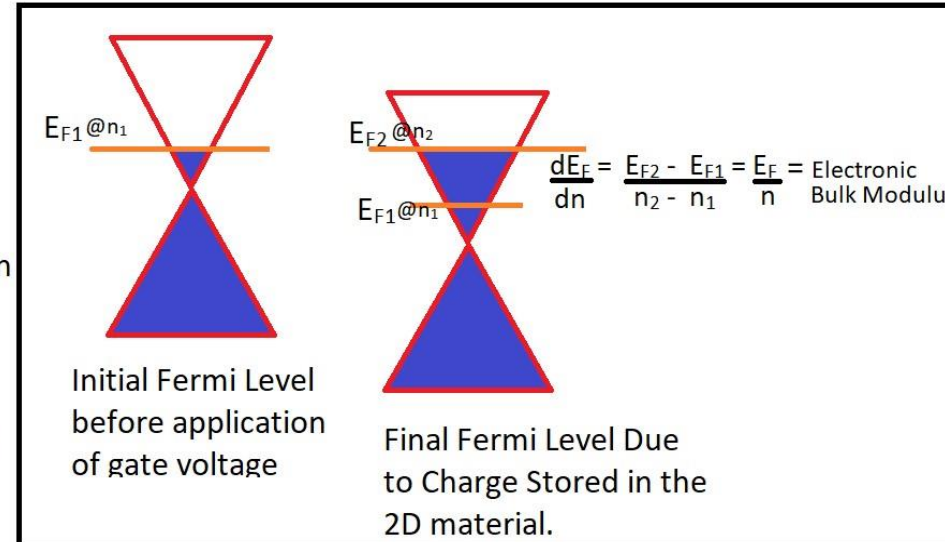
1. To study electron transport in conducting 2D materials.
2. To extract physical Quantities like,
 - Number of Modes.
 - Density Of States.
 - Electronic Compressibility.
 - Energy Band-width.
 - Energy Band-Gap.
 - Carrier Density.
 - Fermi-Energy/Chemical Potential.
 - Fermi Velocity.
 - Ground State and its properties of the 2D materials.
 - Number of Modes.
 - Conductance in the Ballistic and Diffusive Limit.
 - Transmission Function.
 - Mean Free Path.
 - Electron Scattering Mechanisms.
 - Landau Levels and its spacing.
3. To identify whether the 2D material is capable of realizing the Fascinating Outlooks discussed.



QUANTUM CAPACITANCE OF 2D MATERIALS



Band Structure of any 2D material ,Let's consider graphene for example



A diagram showing two parallel plate capacitors connected in series. The top capacitor has a single black circle as its central electrode. The bottom capacitor has two black circles. The voltage across the top capacitor is labeled "V_{across 2D material}". The total charge stored in the 2D material is labeled "Q_{stored in 2D material}".

$$C_{Q,2D} = \frac{Q_{\text{stored in 2D material}}}{V_{\text{across 2D material}}} = \frac{Aen}{\frac{E_F}{e}} = \frac{Ae^2n}{E_F}$$

$$C_{Q,2D} = Ae^2 * \text{Electronic Compressibility}$$

$$C_{Q,2D} = Ae^2 * \text{D.O.S}$$

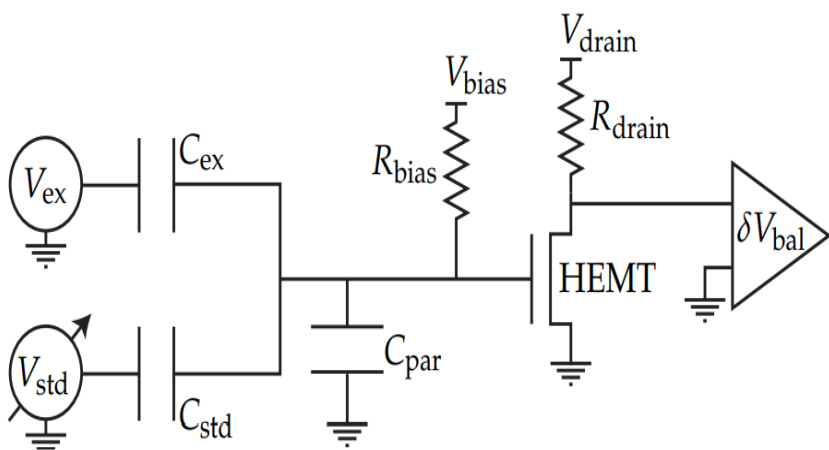
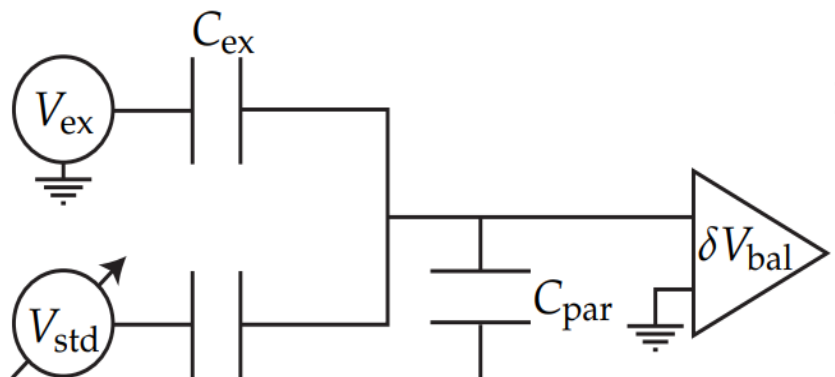
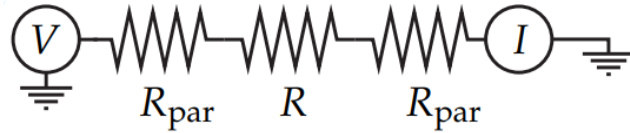


TECHNIQUES OF MEASURING QUANTUM CAPACITANCE OF 2D MATERIALS.

- **Technique 1** - Direct Capacitance Measurement by using a Capacitance Bridge followed by an HEMT to reduce the Parasitic Capacitance.
- **Technique 2** – Extraction of Quantum Capacitance of a top 2D material in a Dielectric-2D material-Dielectric-2D material-Dielectric-SiO₂-Si Van Der Waal Heterostructure with bottom 2D material's Charge Neutrality point acting as a probe.
- **Novel Technique** – Extraction of Quantum Capacitance of 2D material in just Dielectric-2D material-Dielectric-Si-SiO₂ Vander Waal Heterostructure.
- **Raman Spectroscopy's shift in the G and 2D peak** of Graphene with gate voltages can give us idea about the Fermi Energy and the electron carrier concentration from which Quantum Capacitance can be extracted. (only for graphene experimental data is available, for other 2D materials it's field of research.)



TECHNIQUE 1 - DIRECT CAPACITANCE MEASUREMENT



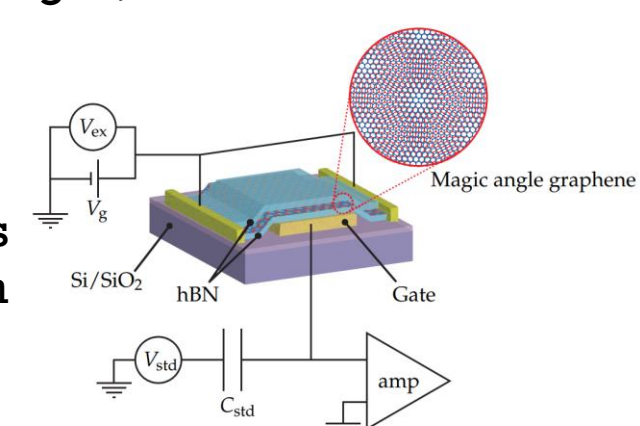
- Equivalent Transport measurement scheme for a capacitor is challenging as most current amplifiers large input impedance above about 10 kHz, limiting currents to about 1 pA for a sample on the order of 1 pF or less for 1 mV source Voltage

$$\delta V_{\text{bal}} = V_{\text{ex}} \frac{C_{\text{ex}}}{C_{\text{ex}} + C_{\text{std}} + C_{\text{par}}} + V_{\text{std}} \frac{C_{\text{std}}}{C_{\text{ex}} + C_{\text{std}} + C_{\text{par}}} = \frac{V_{\text{ex}} C_{\text{ex}} + V_{\text{std}} C_{\text{std}}}{C_{\Sigma}}$$

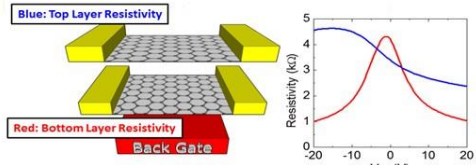
Balance is achieved when, $\delta V_{\text{bal}} = 0 \rightarrow \frac{C_{\text{ex}}}{C_{\text{std}}} = -\frac{V_{\text{std}}}{V_{\text{ex}}}$

But finding balance point in every modulation of gate voltage or magnetic field is difficult so we look at the changes,

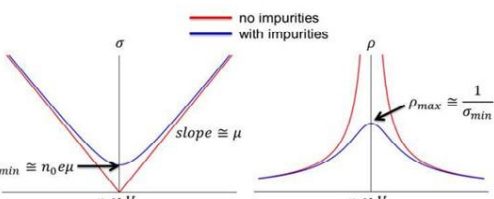
- Use of HEMT reduces the Parasitic Capacitance to 1 pF from 500 pF by decreasing the cable length which is done by shifting the balance point in cryostat, decreases the output impedance.



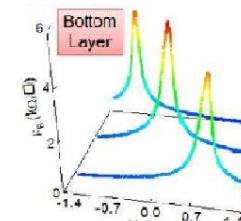
TECHNIQUE 2



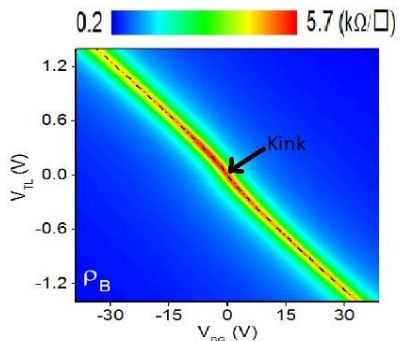
[a] Top layer and Bottom layer Resistivity measured at $T = 300\text{ K}$ (both are monolayer graphene)



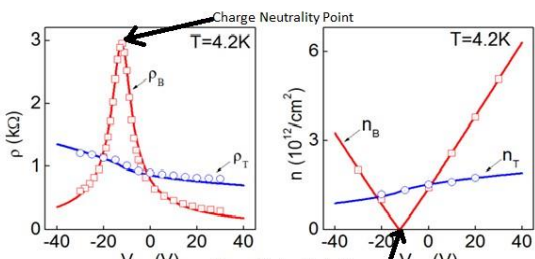
[b] Conductivity and Resistivity Measurements in monolayer graphene with (blue-non ideal substrate) and without charged impurities (ideal substrate)



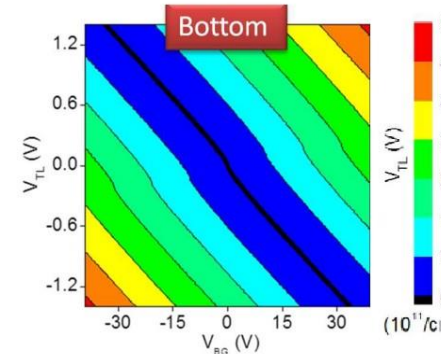
[c] Resistivity measurement of monolayer graphene modulated with V_{BG} and V_{TL}



[d] The charge neutrality line plotted from [c] showing kink in the near zero region V_{BG} and V_{TL} region



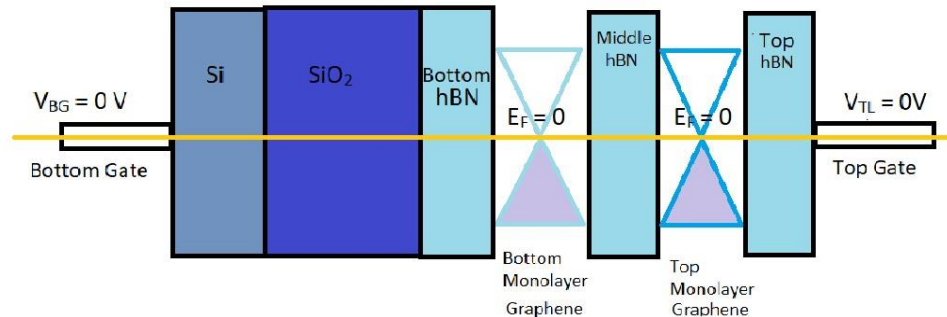
[e] Layer Resistivities and Carrier Densities as a function of V_E measured at $T = 0.4\text{ K}$ indicating the charge neutrality point in the bottom monolayer graphene



[f] Charge Neutrality line Plotted from Band Diagram Calculations with colour indicating the number of carrier density (Excellent Match with the measured Charge neutrality)

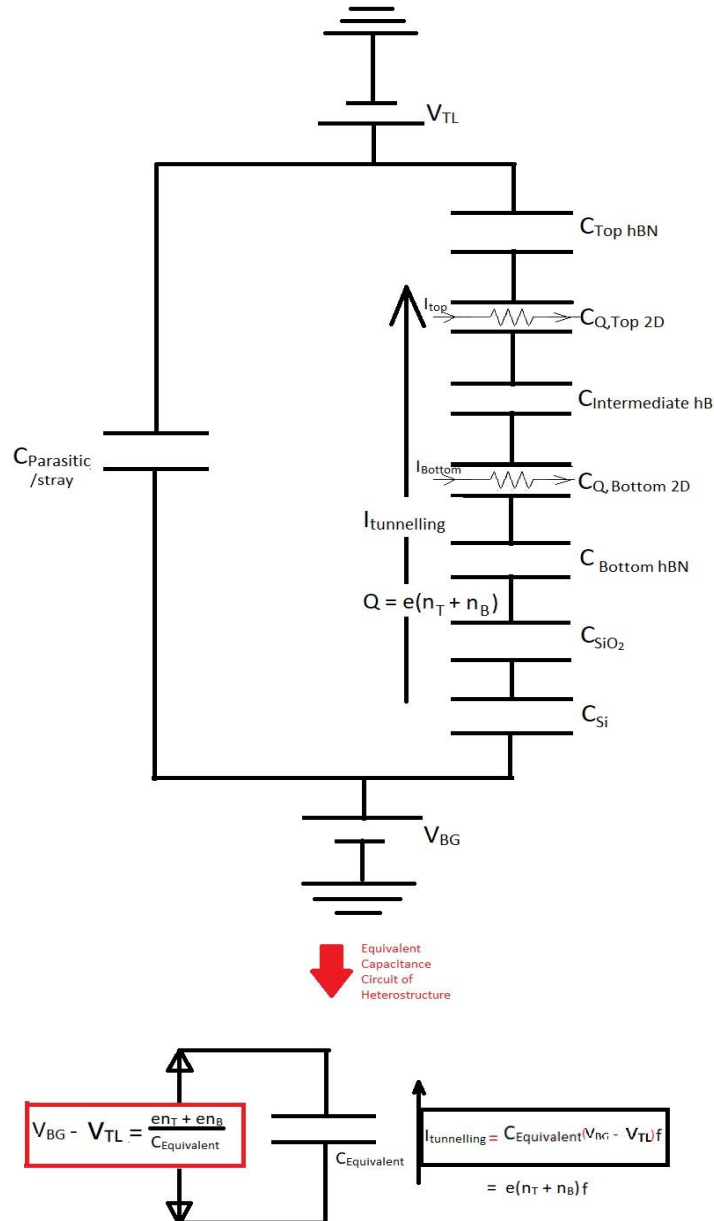


[g] Device Fabrication four probe Design by Gold Contacts eched by electron beam lithography with blue dots marking the contacts taken from the top 2D material and red dots marking the contacts taken from the bottom 2D material



[h] Band Diagram Model in which Fermi Energy, Charge Neutrality and Dirac Point assumed to be coinciding at zero for the two intrinsic monolayers of graphene for zero top and bottom gate voltage in hBN-Mono-hBN-Mono-hBN heterostructure.

TECHNIQUE 2 - CAPACITANCE MODEL OF VAN DER HETEROSTRUCTURE & WHY IT WORKS



By Potential Drop Balance in the Lumped Model,

$$V_{BG} - V_{TL} = \frac{Q_{n_T + n_B}}{C_{Si}} + \frac{Q_{n_T + n_B}}{C_{SiO_2}} + \frac{Q_{n_T + n_B}}{C_{Bottom\ hBN}} + \frac{Q_{n_B}}{C_{Q, Bottom\ hBN}} + \frac{Q_{n_T}}{C_{Intermediate\ hBN}} + \frac{Q_{n_T}}{C_{Q, Top\ hBN}} + \frac{Q^0}{C_{Top\ hBN}}$$

At Charge Neutrality of Bottom Layer, $n_B = 0$

$$V_{BG} - V_{TL} = \frac{en_T}{C_{Si}} + \frac{en_T}{C_{SiO_2}} + \frac{en_T}{C_{Bottom\ hBN}} + \frac{en_B^0}{C_{Q, Bottom\ hBN}} + \frac{en_T}{C_{Intermediate\ hBN}} + \frac{en_T}{C_{Q, Top\ hBN}} \quad \text{A}$$

$$V_{BG} - V_{TL} = \frac{en_T}{C_{Si}} + \frac{en_T}{C_{SiO_2}} + \frac{en_T}{C_{Bottom\ hBN}} + \frac{en_T}{C_{Intermediate\ hBN}} + \frac{en_T}{C_{Q, Top\ hBN}} = en_T \left(\frac{1}{C_{Geo}} + \frac{1}{C_{Q, 2D}} \right) = en_T \left(\frac{1}{C_{Total}} \right)$$

Here, Bottom 2D Material's charge neutrality acts as a breaking Point for the Potential, i.e Potential Drop across Bottom 2D material = 0. Therefore,

$$\begin{aligned} V_{BG} &= \frac{en_T}{C_{Si}} + \frac{en_T}{C_{SiO_2}} + \frac{en_T}{C_{Bottom\ hBN}}, \quad V_{TL} = \frac{en_T}{C_{Intermediate\ hBN}} + \frac{en_T}{C_{Q, Top\ hBN}} \\ \frac{V_{TL}}{V_{BG}} &= \frac{\frac{en_T}{C_{Si}} + \frac{en_T}{C_{SiO_2}} + \frac{en_T}{C_{Bottom\ hBN}}}{\frac{en_T}{C_{Si}} + \frac{en_T}{C_{SiO_2}} + \frac{en_T}{C_{Bottom\ hBN}}} = \frac{\frac{1}{C_{Si}} + \frac{1}{C_{SiO_2}} + \frac{1}{C_{Bottom\ hBN}}}{\frac{1}{C_{Si}} + \frac{1}{C_{SiO_2}} + \frac{1}{C_{Bottom\ hBN}}} \end{aligned}$$

Find $C_{Q, Top}$ from measured n_T which is found by in plane resistivity measurement in top 2D material at charge neutrality voltage gate voltage points of bottom 2D layer

Why this works is specifically because we have a potential breaker in between i.e the charge neutral Bottom 2D material and that is why we can write equation B without requirement to measure the potential drop across the bottom 2D layer as it is zero at charge neutrality.

But if we carefully look at equation A then we can't assume, $(V_{BG} - V_{TL}) \propto n_T$

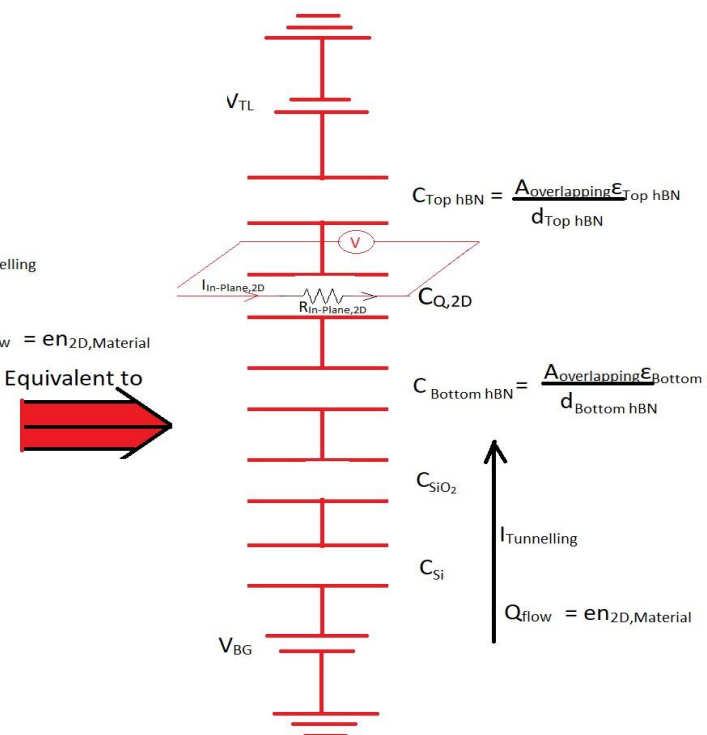
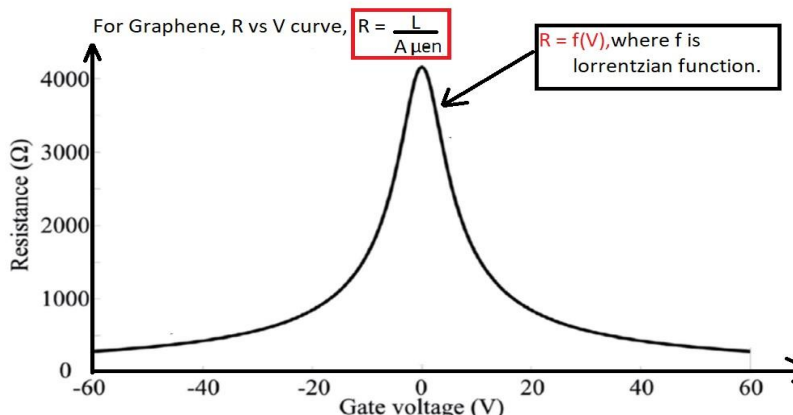
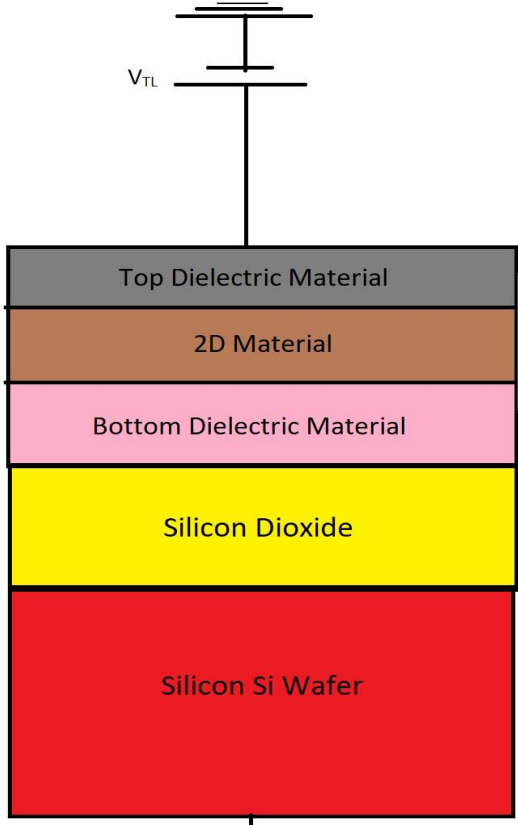
Because if we do that then, $(V_{BG} - V_{TL}) = Kn_T$, where K is constant of proportionality

$$Kn_T = \frac{en_T}{C_{Si}} + \frac{en_T}{C_{SiO_2}} + \frac{en_T}{C_{Bottom\ hBN}} + \frac{en_T}{C_{Intermediate\ hBN}} + \frac{en_T}{C_{Q, Top\ hBN}}$$

Now if we look at equation B it totally cancels the top carrier density from the equation and we can exactly estimate the quantum capacitance for modulation of top gate and bottom gate voltages as we know its set values and equation B is possible to write with only one unknown term ($C_{Q, Top}$) because of the charge neutrality of the bottom 2D material, hence it has no potential difference across it and hence its unknown term directly becomes zero. And for each top and bottom voltage points of these charge neutralities we can find the top carrier density n_T by in plane resistivity measurement from the relation $\sigma_{measured} = \mu en_T$

$C_{Q, Top} = \text{const with variation of } n_T$ and we know that from definition of Quantum Capacitance that C_Q varies with n_T hence the assumption is wrong, as we are in short assuming total capacitance equal to constant geometric capacitance and ignoring the quantum capacitance

NOVEL TECHNIQUE FOR PROBING QUANTUM CAPACITANCE



By Potential Voltage Balance across 2D Hetero-structure,

$$V_{BG} - V_{TL} = \frac{en}{C_{Si}} + \frac{en}{C_{SiO2}} + \frac{en}{C_{Bottom\ hBN}} + \frac{en}{C_{Q,2D}}$$

We know, $\sigma = \mu en$, if ohm's law is satisfied ignoring scattering and defects in the 2D material

$R_{in-plane}$ we are going measure by passing an in plane current and measuring the in plane longitudinal voltage. From R we can get the in plane resistivity by $\rho = R_{in-plane} A/s = \frac{1}{L} \mu en$

Now,we can write , the equivalent total capacitance as $C_T(V_{BG} - V_{TL}) = C_Q(V_{across\ 2D\ material}) = \frac{C_Q e_F}{e} = en = C_{Geo} V_{across\ geo}$

Now if we assume $C_T(V_{BG} - V_{TL}) \approx C_{Geo}(V_{BG} - V_{TL}) = en$, we are ignoring the changes of Quantum Capacitance vs n

As if we assume this is the case i.e $(V_{BG} - V_{TL}) = \frac{en}{C_{Geo}}$

$$\frac{en}{C_{Geo}} = \frac{en}{C_{Si}} + \frac{en}{C_{SiO2}} + \frac{en}{C_{Bottom\ hBN}} + \frac{en}{C_{Q,2D}} \rightarrow C_{Q,2D} = \text{const} = 0$$

Let us consider it varies as $R = \frac{1}{1 + v^2}$

$$\frac{L}{A \mu en} = \frac{1}{1 + v^2} \rightarrow n = \frac{L(1 + v^2)}{A \mu en}$$

$$V = en \left(\frac{1}{C_{Si}} + \frac{1}{C_{SiO2}} + \frac{1}{C_{Bottom\ hBN}} + \frac{1}{C_{Q,2D}} \right)$$

$$\frac{V}{L(1 + v^2)} = \left(\frac{1}{C_{Si}} + \frac{1}{C_{SiO2}} + \frac{1}{C_{Bottom\ hBN}} + \frac{1}{C_{Q,2D}} \right)$$

$\frac{L}{A \mu}$ = Scaling Factor = 1

$$\frac{V}{1 + v^2} = \left(\frac{1}{C_{Si}} + \frac{1}{C_{SiO2}} + \frac{1}{C_{Bottom\ hBN}} + \frac{1}{C_{Q,2D}} \right)$$

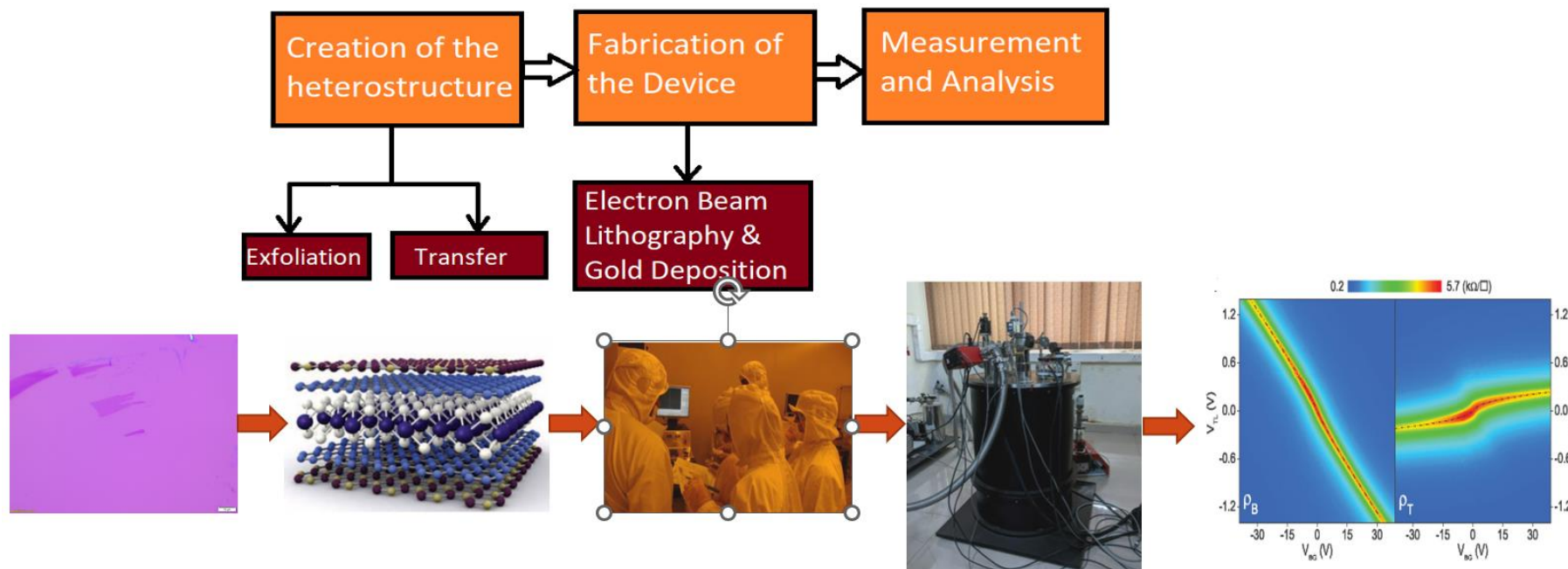
$$\frac{V}{1 + v^2} = \left(\frac{1}{C_{Geo}} + \frac{1}{C_{Q,2D}} \right) \rightarrow \text{Find } C_{Q,2D} \text{ for each value of } V$$

Plot $C_{Q,2D}$ for each value of n ,but since we have taken the scaling factor to be 1 we cannot exactly know the value of $C_{Q,2D}$ in Farads so we can take the Length, Area of cross section from our heterostructure and carrier mobility from previous measured sample (or Hall Measurements)



EXPERIMENTAL PROCEDURES INVOLVED/WORKFLOW

- Exfoliation of 2D materials.
- Characterization of 2D materials – 6 Methods and what does each one can characterize for 2D materials with Raman and Optical Microscopy technique being discussed in detail.
- Dry Transfer Techniques
- Device Fabrication
- Measurement – 1. With Magnetic field and
2. Without Magnetic field.



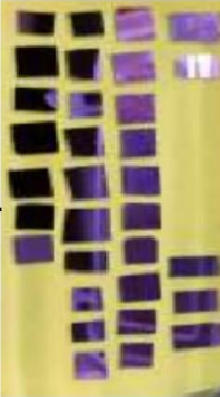
EXFOLIATION OF 2D MATERIALS



[a] Remove Silicon Wafer from Dessicator



[b] Cut the Silicon Wafers in small squares by Pencil Cutter



[c] Small Cut Squares of Silicon Wafer



[d] Dip the Silicon Wafer in Acetone taken in Petri Dish



[e] Ultrasonicate the Silicon Wafer with Acetone



[j] Repeat the procedure until one gets uniform density distribution of the graphene flakes



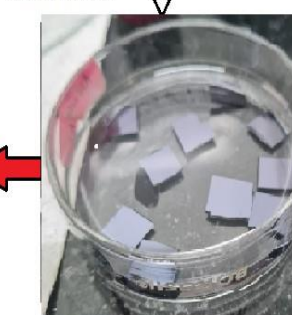
[i] Peel off the graphite flake on scotch tape by sticking and unsticking the scotch tape



[h] Take the graphite flake on Scotch Tape



[g] Plasma O₂ treat the Silicon Wafer



[f] Clean the Silicon Wafer by using IPA and then blow dry it using N₂



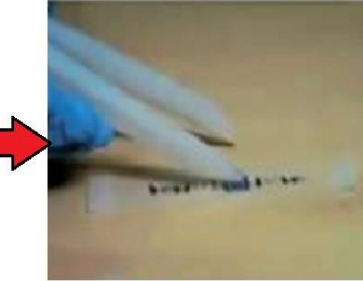
[k] Repeat the procedure until one gets uniform density distribution of the graphene flakes



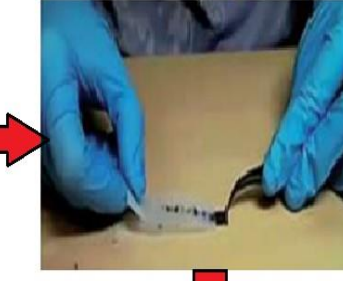
[l] Uniform density distribution of the graphene flakes on scotch master tape



[m] Copying the master tape flakes on another flakes by sticking and unsticking of master tape with another tape



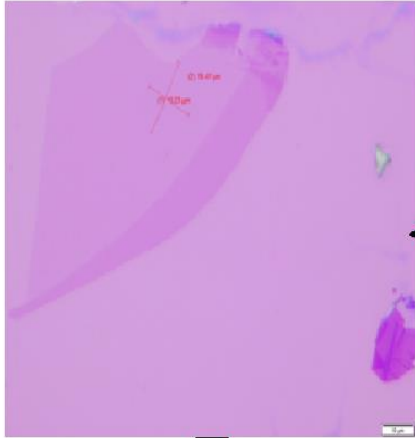
[n] Sticking the Silicon Wafer on the scotch tape



[o] Applying Pressure on Silicon Wafer adhesed to scotch tape to get uniform adhesion



EXFOLIATION AND TRANSFER SETUP OF 2D MATERIALS CONTINUED



[t] Observing the monolayer flake due to optical contrast on the microscope



[s] Optically checking each substrate for graphene with optical zooming power varying from 5x to 100x.



[r] Putting the Graphene Exfoliated silicon wafer in sticky taped bottom box for sticking the Silicon oxide substrate to the box



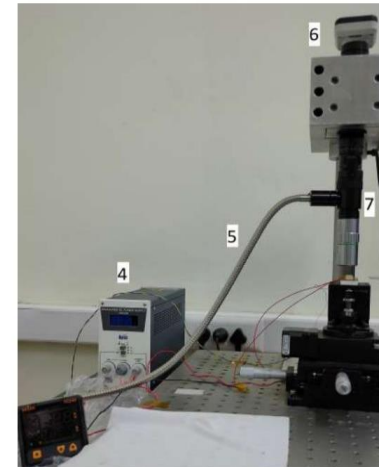
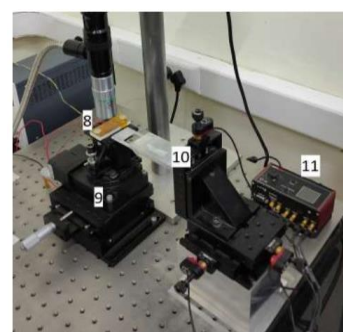
[q] Air cooling the Substrate and then removing the scotch tape gently



[p] Heating the Silicon Wafer with scotch tape attached to 100 C for increasing the adhesion energy of substrate with monolayer graphene



[u] Putting the box containing Silicon wafers back in the dessicator and then vacuumizing it to avoid air contamination

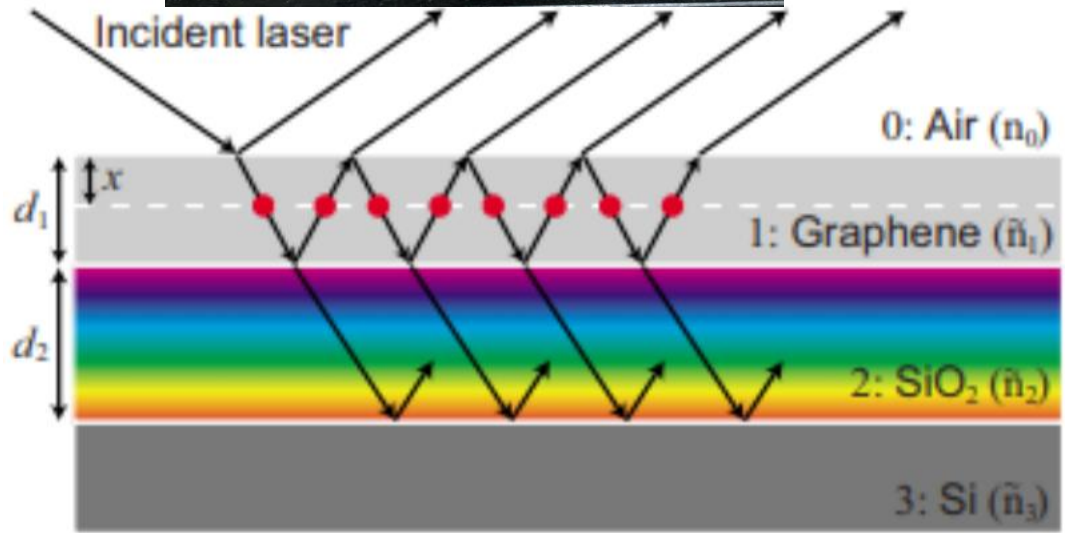


The transfer setup consists of the following parts:

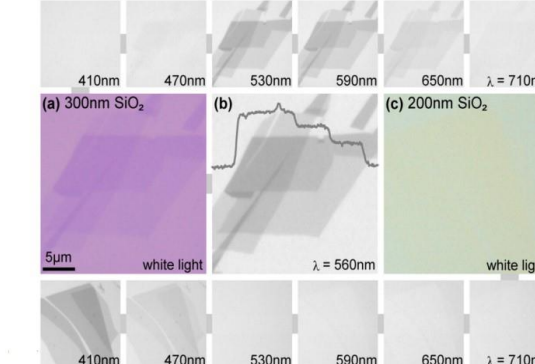
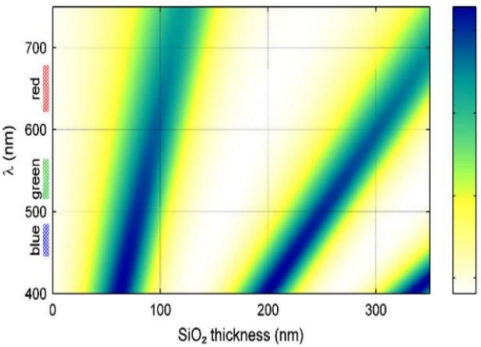
1. OSL2 fiber illuminator: provides illumination for the microscope stage
2. Micro position controller: power source of the rotation stage
3. PID temperature controller: heats the stage
4. Regulated DC power supply: provides voltage to the temperature controller
5. Optical cable: connects illuminator to the microscope
6. Moticam camera: used to see and capture samples under the microscope
7. Optical microscope: has 20x magnification with up to 4x zoom
8. Microscope stage: holds the substrate and has an integrated heater
9. Motorized twist stage: used in twisted bilayer stack making
10. Transfer component: contains an aluminium plate and Piezo actuators
11. Piezo motor controller: powers Piezo actuators

CHARACTERIZATION OF 2D MATERIALS

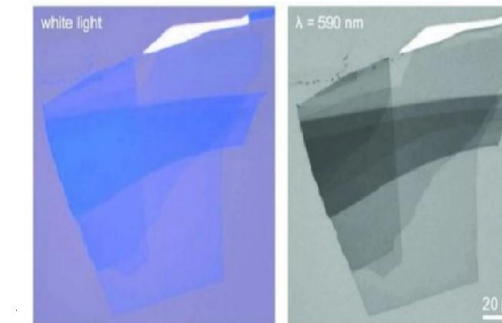
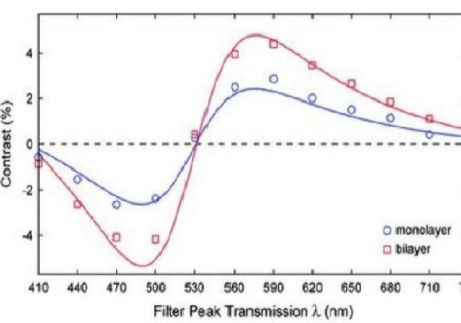
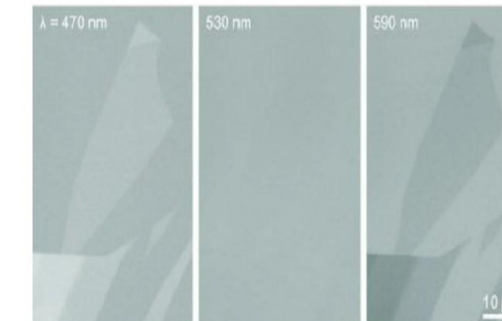
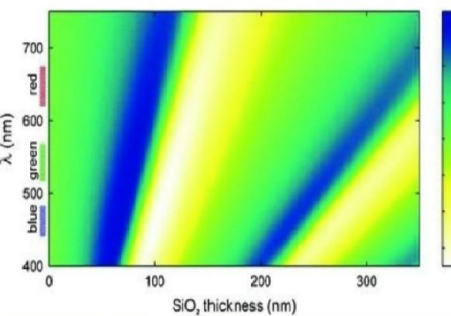
■ Optical Microscopy



[a] Graphene

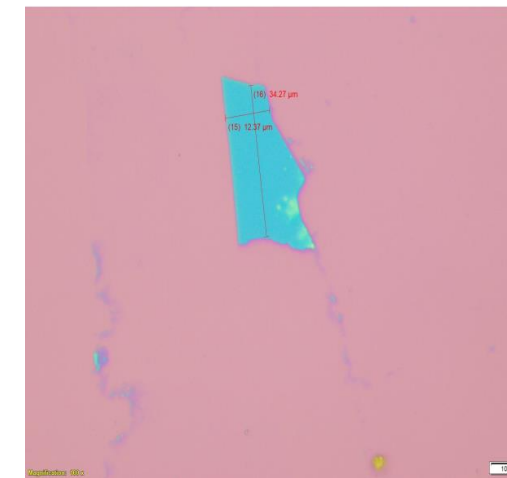
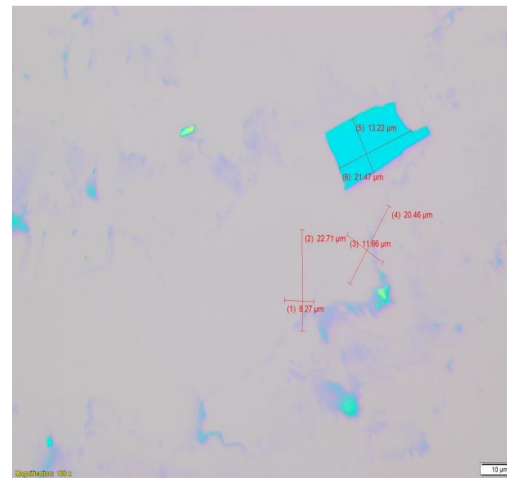
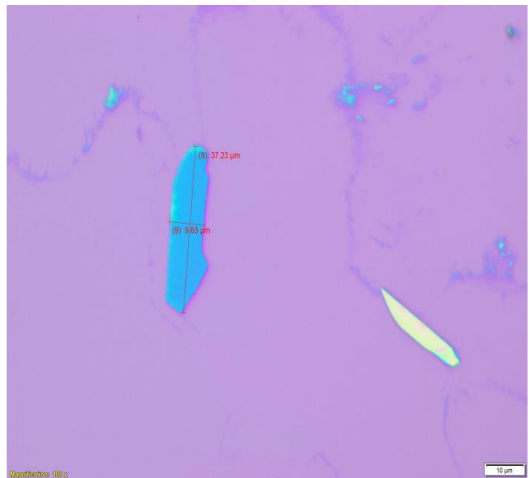
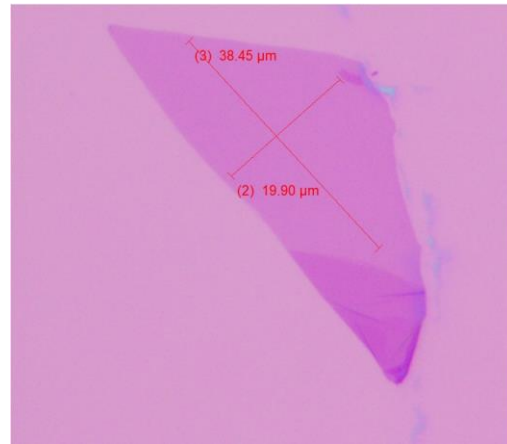
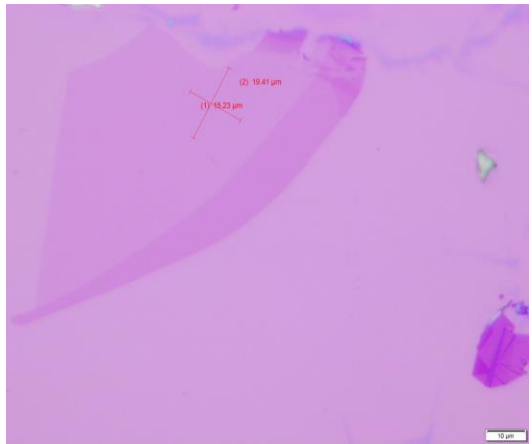


[b] hBN



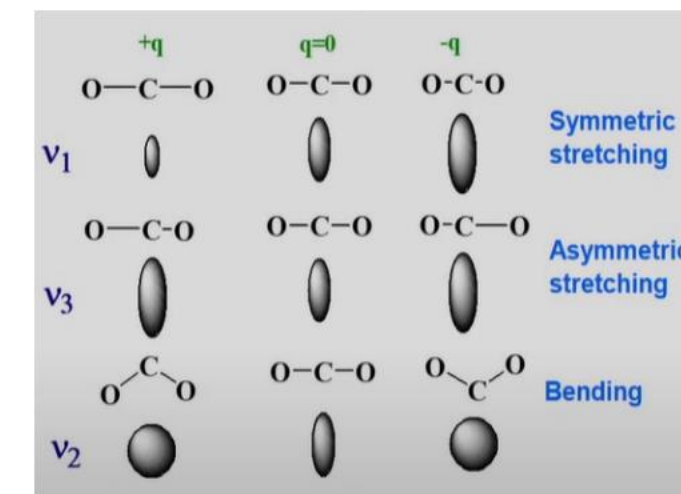
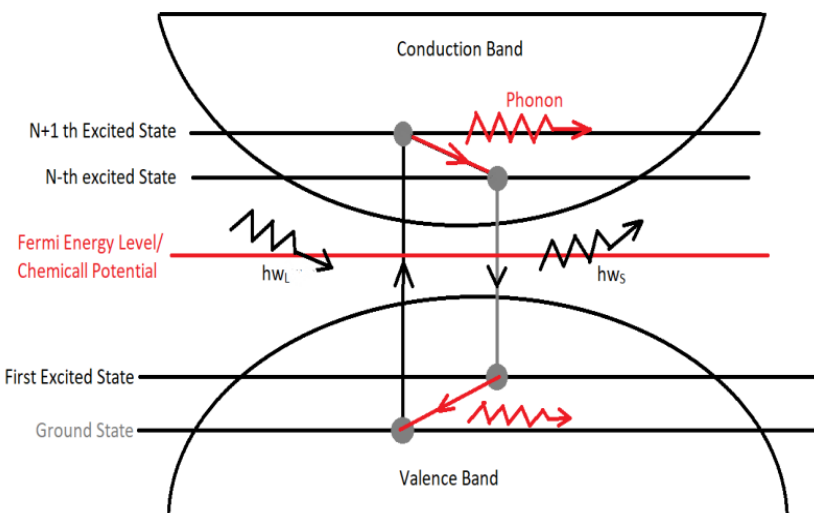
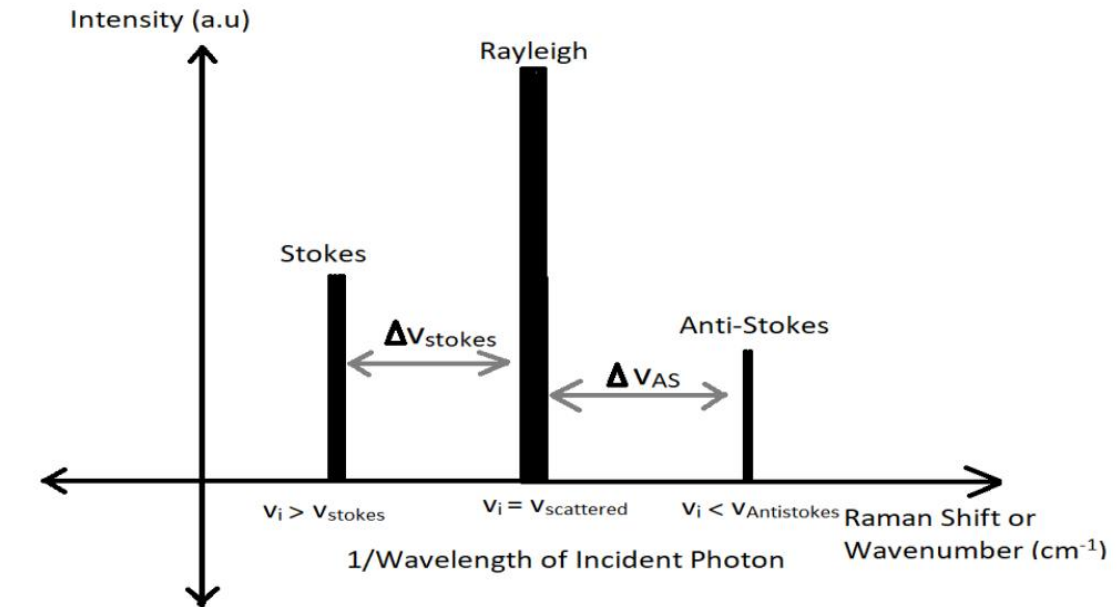
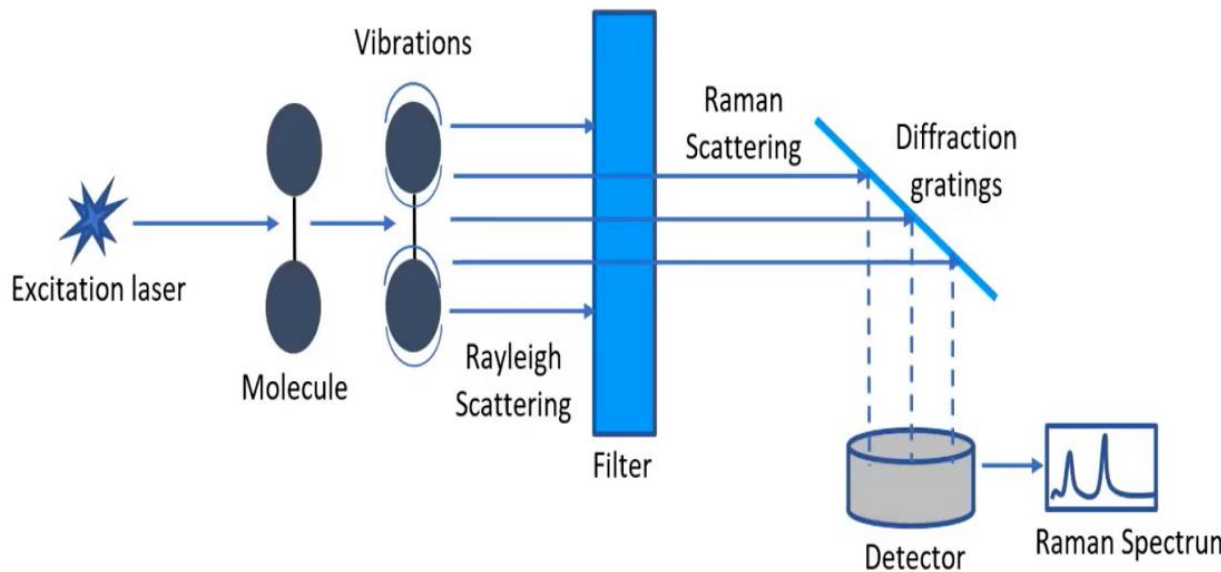
CHARACTERIZATION OF 2D MATERIALS (CONTINUED)

- Optical Microscopy (Images of Graphene and hBN flakes for the stack)



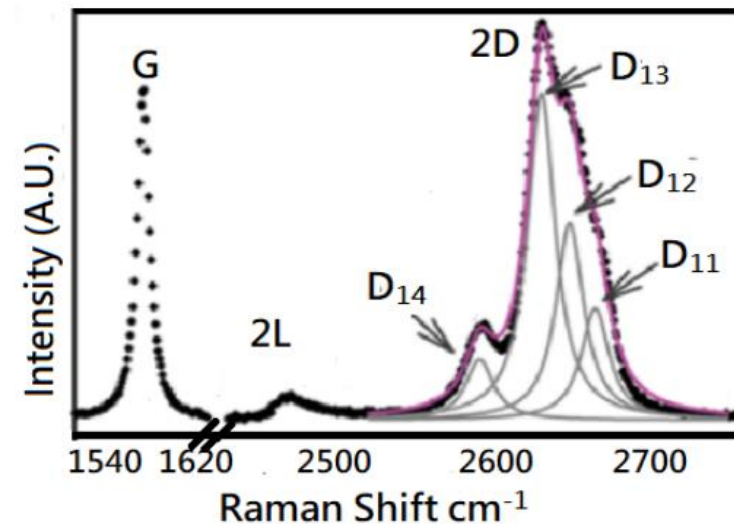
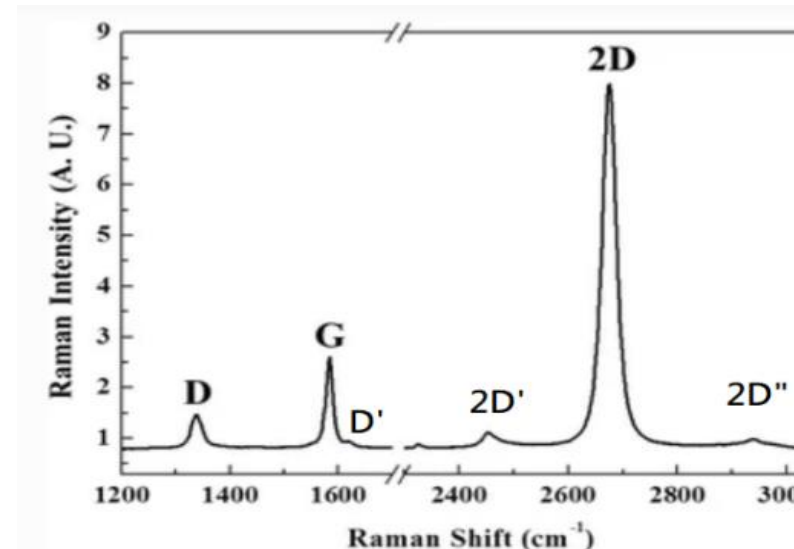
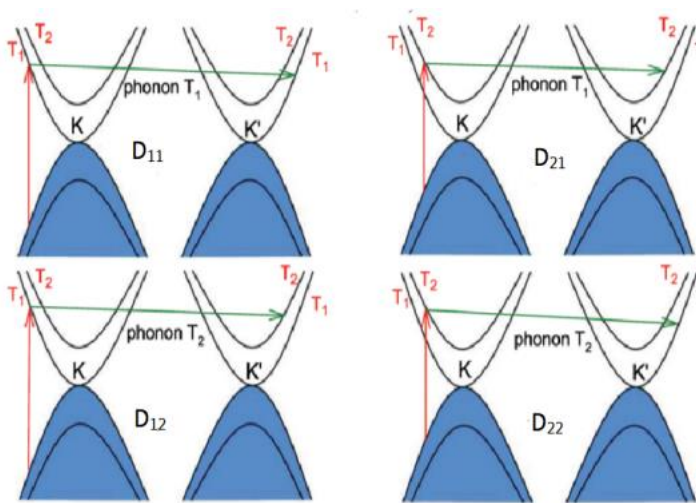
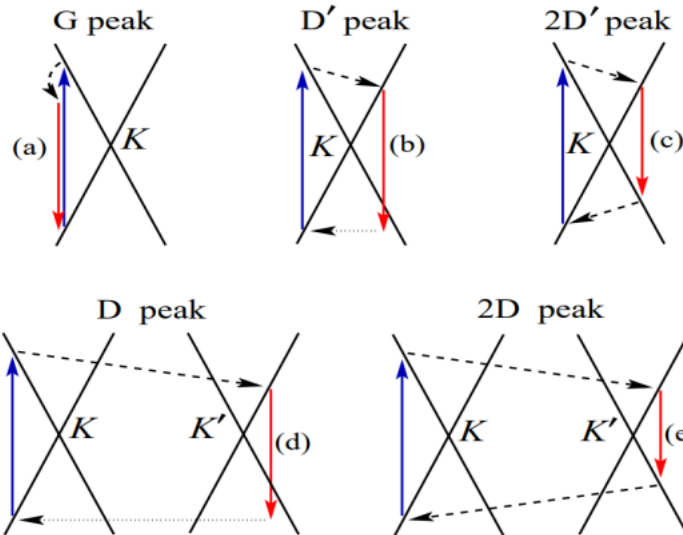
CHARACTERIZATION OF 2D MATERIALS (CONTINUED)

▪ Raman Spectroscopy Basics



CHARACTERIZATION OF 2D MATERIALS (CONTINUED)

■ Raman Spectroscopy of Monolayer Graphene and Bilayer Graphene explanation from Band Diagram



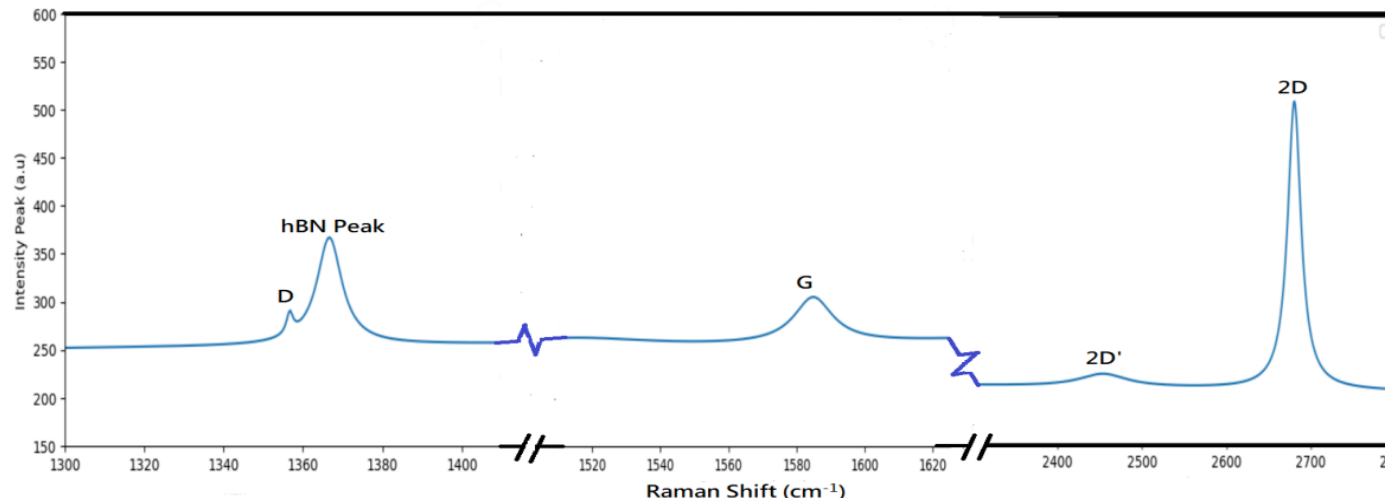
.Wu, Jiangbin Lin, Miao-Ling Xin, Cong Liu, Henan Tan, Ping-Heng. (2018). Raman spectroscopy of graphene-based materials and its applications in related devices. *Chemical Society Reviews*. 47. 10.1039/C6CS00915H.

Basko, D. Piscanec, S. Ferrari, A. (2009). Electron-electron interactions and doping dependence of the two-phonon Raman intensity in graphene. *Physical Review B*. 80. 10.1103/PhysRevB.80.165413.

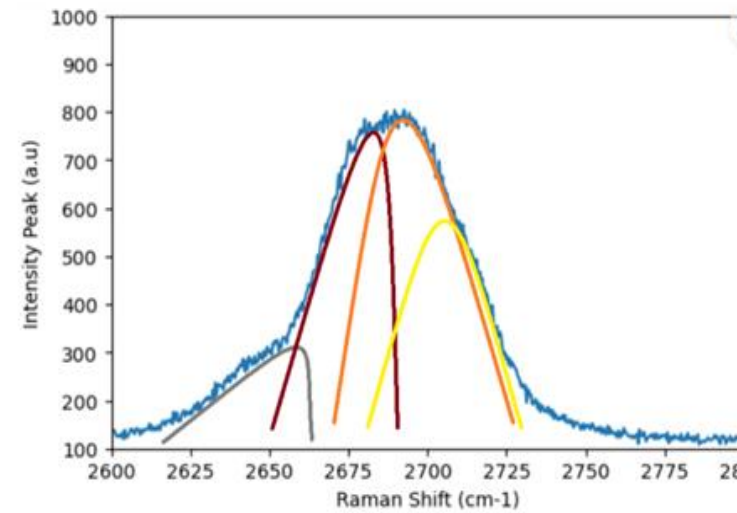
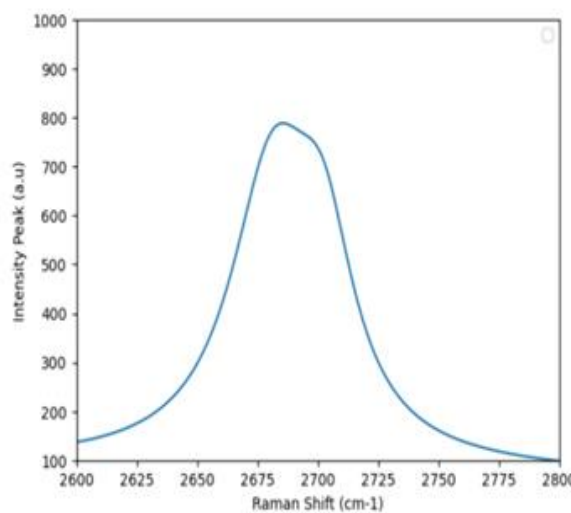
.Heo, Gaeun Kim, Yong Chun, Seung-Hyun Seong, Maeng-Je. (2015). Polarized Raman spectroscopy with differing angles of laser incidence on single-layer graphene. *Nanoscale Research Letters*. 10. 10.1186/s11671-015-0743-4.

CHARACTERIZATION OF 2D MATERIALS (CONTINUED)

- Raman Spectroscopy of Monolayer Graphene and Bilayer Graphene for My sample at 532 nm i.e 2.33 eV Laser Source



- D peak at 1356 cm^{-1} , G peak at 1585 cm^{-1} , 2D peak at 2680 cm^{-1} , 2D' peak at 2450 cm^{-1} , hBN peak at 1366 cm^{-1} with 100 mW incident power at room temperature with 10 percent notch filtering (50 cm^{-1})



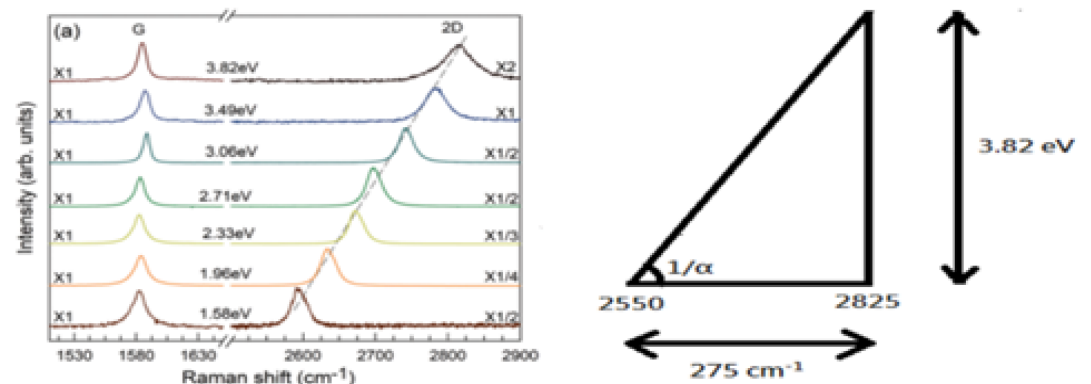
- Four D peaks observed as expected for Bilayer Graphene characterizing the number of graphene layers as two in number



CHARACTERIZATION OF 2D MATERIALS (CONTINUED)

- Quantities that can be extracted from Raman Spectra of monolayer Graphene by comparing it previous experimental data from papers.

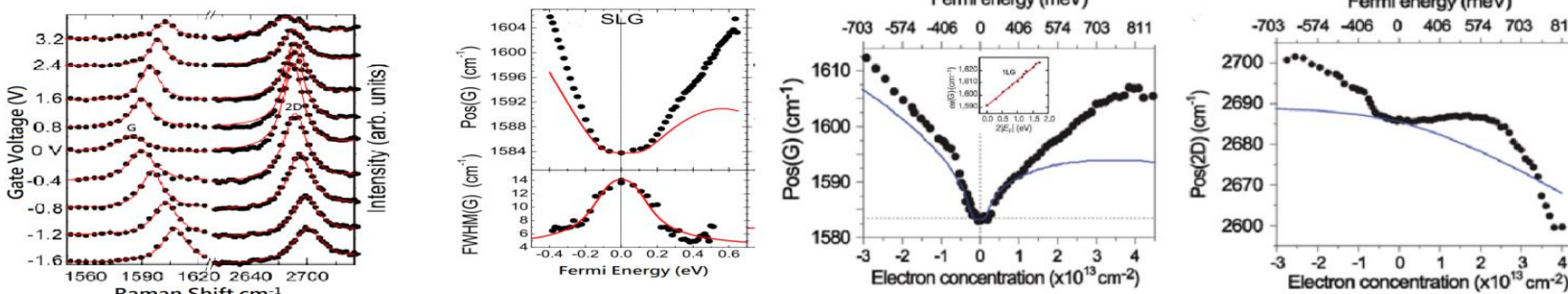
1. Extrapolation of Raman Shift of 2D peak of Monolayer Graphene from Previous Experimental Raman Spectra Data for different Excitation Lasers



- Excitation Energy of Laser = Slope \times Raman Shift(2D) + Constant
- For a 2.33 eV excitation laser, Raman Shift(2D) = 2717.78 cm^{-1} indicating an overfit of the data as the 2D peak is observed at 2680 cm^{-1}

2. Extracting the Fermi Energy and carrier concentration.

• 1st Way – By Previous Experimental Plots for Monolayer Graphene



- The Position of the G and 2D peak of the Raman Spectra for our sample is at 1585 cm^{-1} and 2680 cm^{-1} respectively.
- The FWHM of the G peak is around 11 cm^{-1} . Hence extrapolating the Fermi Energy for our single layer graphene sample we get $E_F = 0.15 \text{ eV}$, $n = 0.25 \times 10^{13} \text{ per cm}^{-2}$.

Gorbachev, Roman Riaz, Ibtam Raveendran-Nair, Rahul Jalil, Rashid Britnell, Liam Belle, B. Hill, Ernie Novoselov, K. Watanabe, K. Taniguchi, Takashi Geim, A. Blake, P. (2010). Hunting for Monolayer Boron Nitride: Optical and Raman Signatures.

Xin, Cong Wu, Jiangbin Lin, Miao-Ling Xueli, Liu Shi, Wei Venezuela, Pedro Tan, Ping-Heng. (2018). Anti-Stokes Raman scattering in mono- and bilayer graphenes. *Nanoscale*. 10. 10.1039/C8NR04554B.

Wu, Jiangbin Lin, Miao-Ling Xin, Cong Liu, Henan Tan, Ping-Heng. (2018). Raman spectroscopy of graphene-based materials and its applications in related devices. *Chemical Society Reviews*. 47. 10.1039/C6CS00915H.

Das, A Chakraborty, Biswanath Piscanec, S. Pisana, S. Sood, A. Ferrari, A. (2008). Phonon renormalisation in doped bilayer graphene. *Phys Rev B*. 79

CHARACTERIZATION OF 2D MATERIALS (CONTINUED)

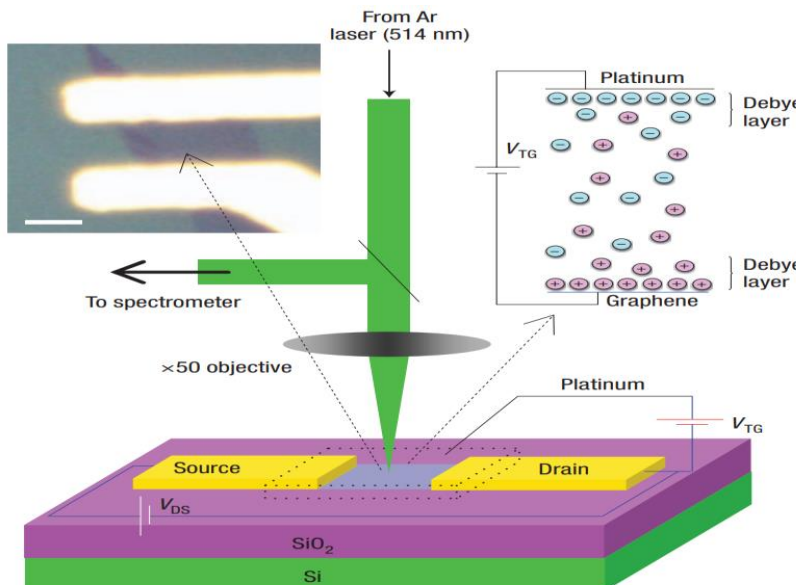
- 2nd Way – The relation between ratio of the peak area intensity of the G and the 2D peak with the Fermi Energy by considering electron-electron interactions,

$$\sqrt{\frac{A(G)}{A(2D)}} = C' [\gamma_{e-ph} + |E_F| f(e^2/\epsilon v_f)]$$

By Potential Balance,

$$V_G = \frac{E_F}{e} + \phi \rightarrow V_{TG} = \frac{\hbar |\nu_F| \sqrt{\pi n}}{e} + \frac{ne}{C_{TG}}$$

$$V_{TG} (\text{volts}) = 1.16 \times 10^{-7} \sqrt{n} + 0.723 \times 10^{-13} n$$



, where γ_{e-ph} is the electron – phonon scattering rate which can be found from the Raman Excitation Time of the electron which is in orders of 10^{-14} s. And ϵ is the dielectric constant of the dielectric used between source and Drain in the experimental setup described below.

3. Fermi Velocity of Graphene –

$$v_f = \frac{E_F}{\hbar \sqrt{\pi n}} = 0.8116 \times 10^6 \text{ m/s}$$

4. Phonon Velocity of Scattering

The phonon velocity by using the change in 2D peak frequency for Raman Stokes and Antistokes and the Energy of Excitation slope with Raman Shift of stokes 2D peak,

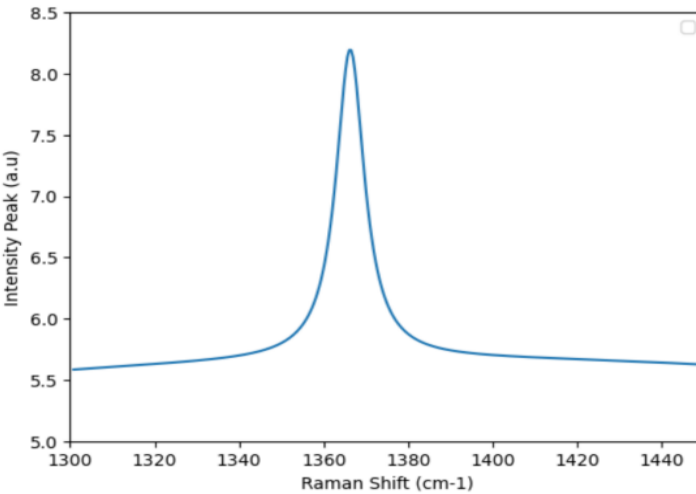
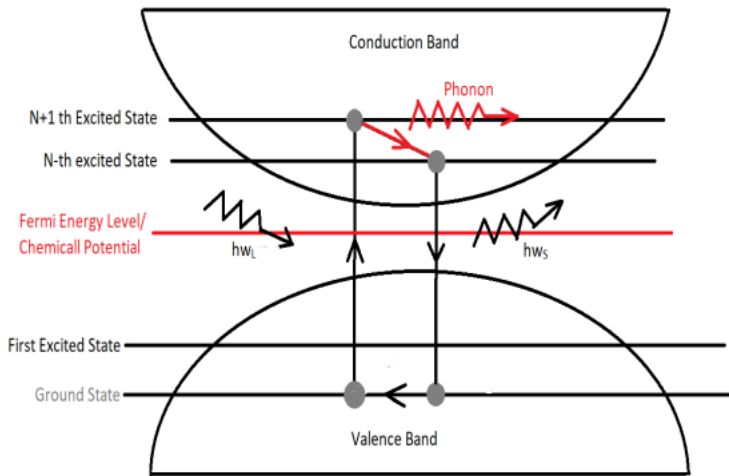
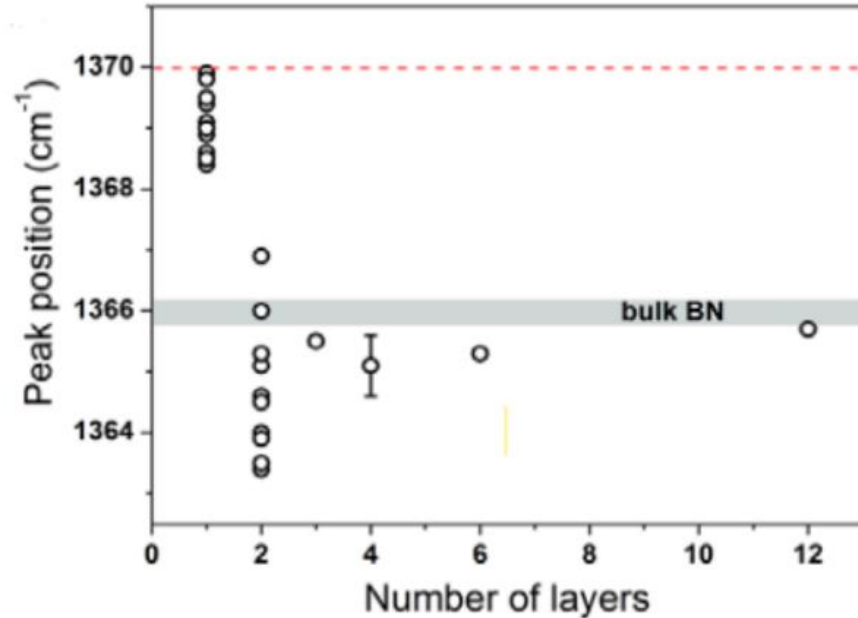
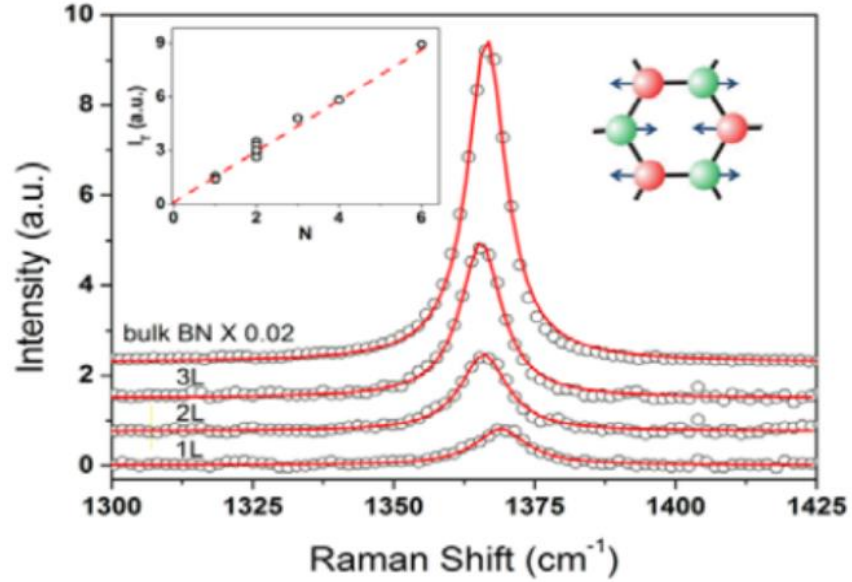
$$v_{ph} = \frac{\alpha_s/2}{1-\alpha_s/2} v_f = \frac{0.01/2}{1-0.01/2} v_f = \frac{0.005}{0.995} v_f = 4078.39 \text{ m/s}$$

$$\text{where, } 1/\alpha_s = \frac{1}{\tan(1/\alpha)} = 100 \frac{\text{cm}^{-1}}{\text{eV}} \text{ (ideal linear fit)}$$

5. Number of Layers of Graphene

can also be extracted from previous experimental plot of Intensity Ratio of G peaks of N layered Graphene to single layer graphene vs the number of layers of Graphene.

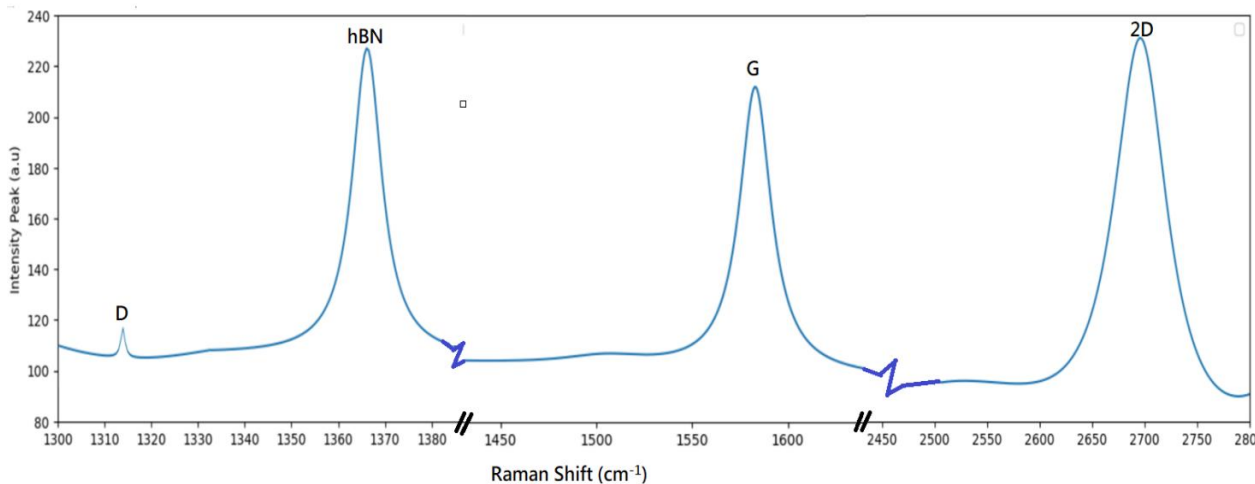
RAMAN SPECTROSCOPY OF HEXAGONAL BORON NITRIDE



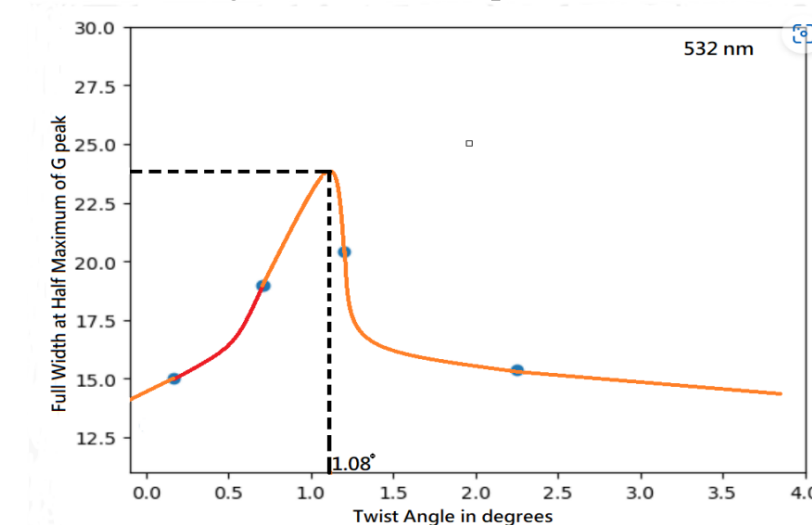
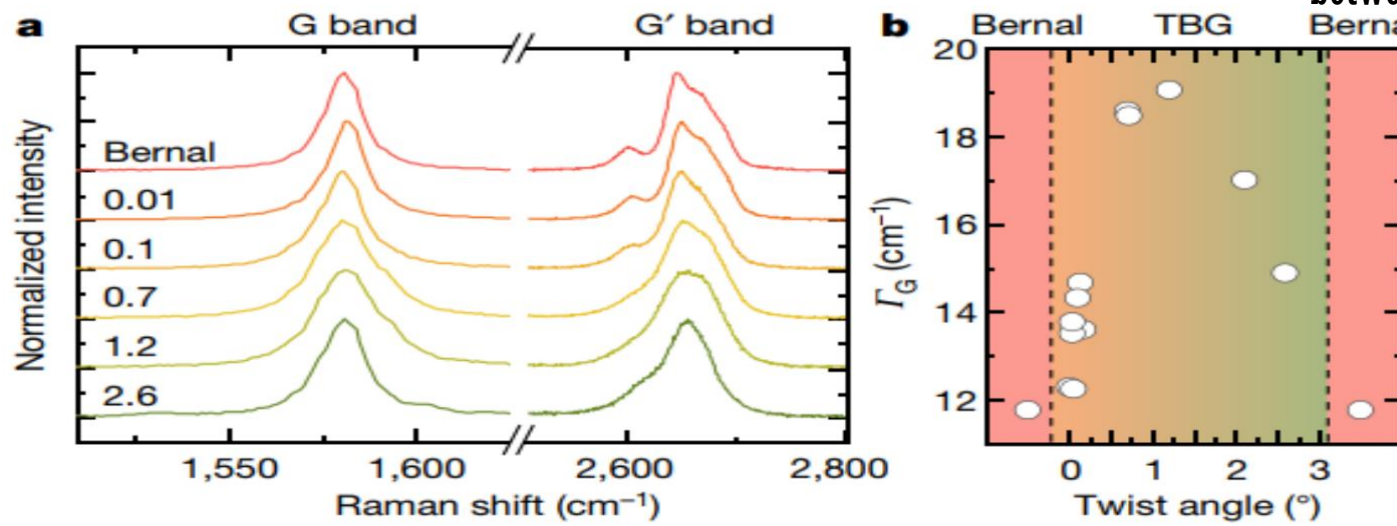
- Raman Peak at 1366 cm^{-1} for my hBN sample is observed in the plot indicating that the number of layers of hBN is between 5 to 12 , but less than 12.



RAMAN SPECTROSCOPY OF TBG TO DETERMINE THE ANGLE OF TWIST – 532 NM LASER SOURCE



- D peak at 1315 cm^{-1} , hBN peak at 1366 cm^{-1} , G peak at 1585 cm^{-1} , 2D peak at 2695 cm^{-1} and FWHM of G peak is 20.25 cm^{-1} to 21.2 cm^{-1} .
- At magic angle i.e 1.08° , as there is flattening of bands, there is an increase in density of states at zero Fermi Energy, hence the Raman Shift of the scattered photon can be in a range (with this range increasing to maximum as we approach magic angle) near to G peak and hence there is broadening of the G peak i.e FWHM of the G peak increases near magic angle and is max at 1.08° twist angle.
- FWHM of G peak is 20.25 cm^{-1} to 21.2 cm^{-1} indicating Twist Angle is in between 0.8 to 1.15 degrees of our sample



Gadelha, Andreij Ohlberg, Douglas Rabelo, Cassiano Silva, Eiel Vasconcelos, Thiago Campos, Joao Luiz Lemos, Jéssica Ornelas, Vinícius Miranda, Daniel Nadas, Rafael Santana, Fabiano Watanabe, Kenji Taniguchi, Takashi Van Troeye, Benoit Lamparski, Michael Meunier, Vincent Nguyen, Viet-Hung Paszko, Dawid Charlier, Jean-Christophe Jorio, Ado. (2021). Localization of lattice dynamics in low-angle twisted bilayer graphene. *Nature*. 590. 405-409. 10.1038/s41586-021-03252-5.

Campolina, Tiago Gadelha, Andreij Ohlberg, Douglas Watanabe, Kenji Taniguchi, Takashi Medeiros-Ribeiro, Gilberto Jorio, Ado Campos, Leonardo. (2022). Raman spectra of twisted bilayer graphene close to the magic angle.

CHARACTERIZATION OF 2D MATERIALS (SUMMARY)

- **Angle Resolved Photoemission Spectroscopy.**

- Actual many body interactions band Structure of 2D material.

- **Optical Microscopy.**

- Visually see graphene and BN contrast on Si – SiO₂ substrate and identify the number of layers from contrast observed.

- **Scanning Electron Microscopy.**

- Number of Graphene layers and surface defects.

- **Transmission Electron Microscopy.**

- Characterization of Defects (Point , Dislocation , Grain Boundaries etc.)

- Type of Graphene edges => Zigzag , Armchair , Klein Edge.

- Number of layers of Graphene.

- **Scanning Probe Microscopy and Atomic Force Microscopy**

- Height of Graphene , hBN Flakes, Work Potentials , Charge Impurities in the 2D material.

- Landau Levels by Conductance Measurements , Lattice Mismatch , AFM Lithography.

- Quality of CVD grown graphene by K.P.M

- **Raman Spectroscopy**

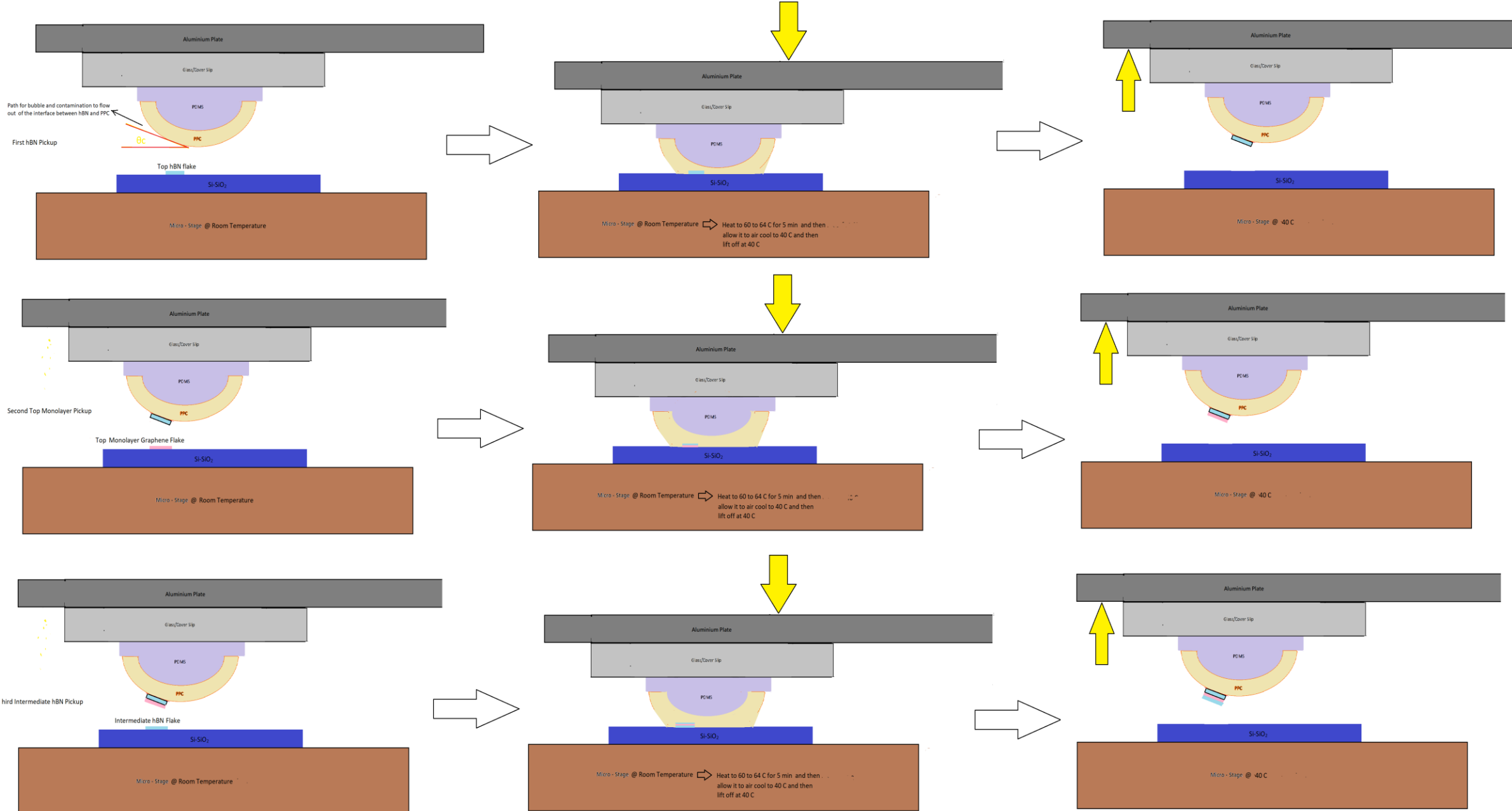
- Number of layers of graphene , Defects , Quality of CVD

- Phonon Velocity , Fermi Energy , Twist Angle of Twisted Bilayer Graphene

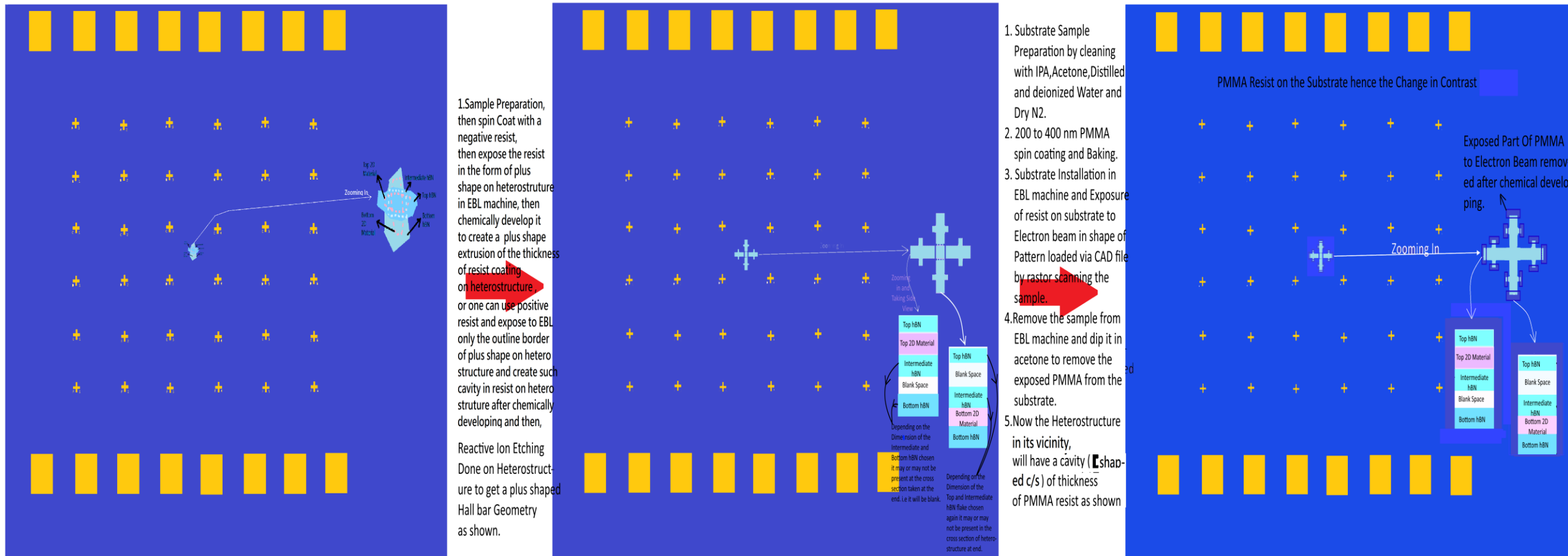
- Quantum Capacitance of only Graphene



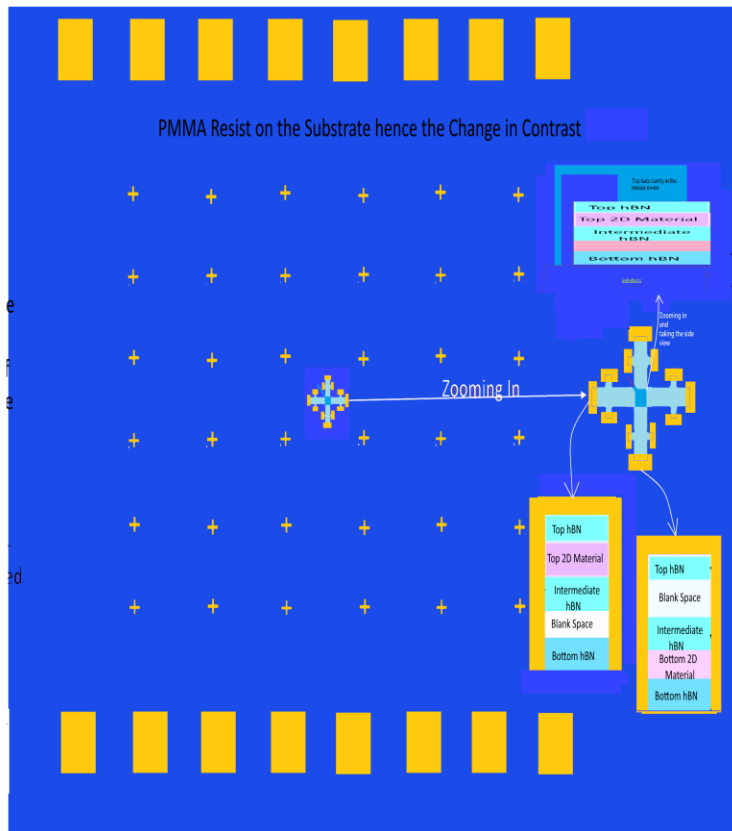
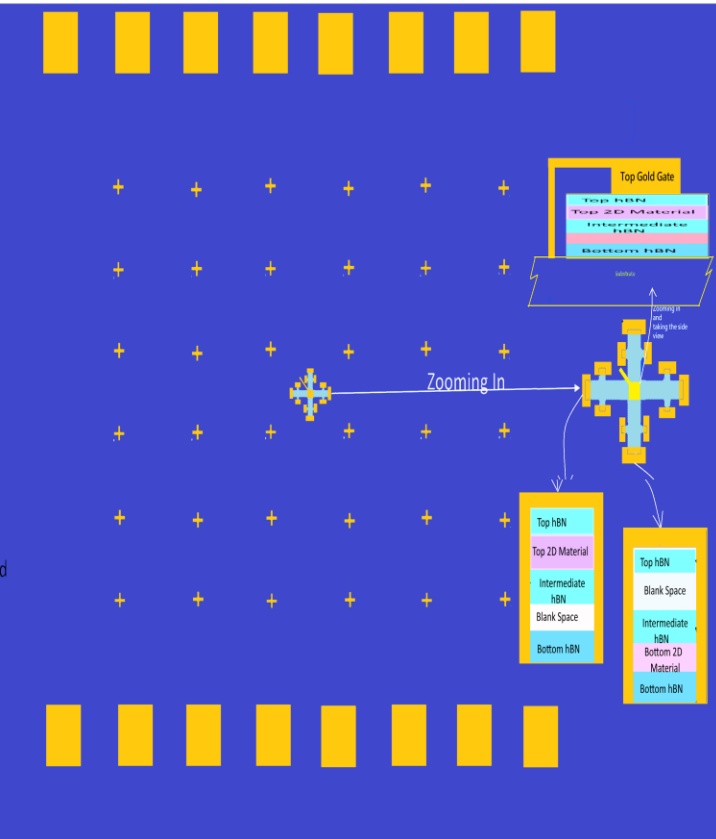
DRY TRANSFER TECHNIQUE



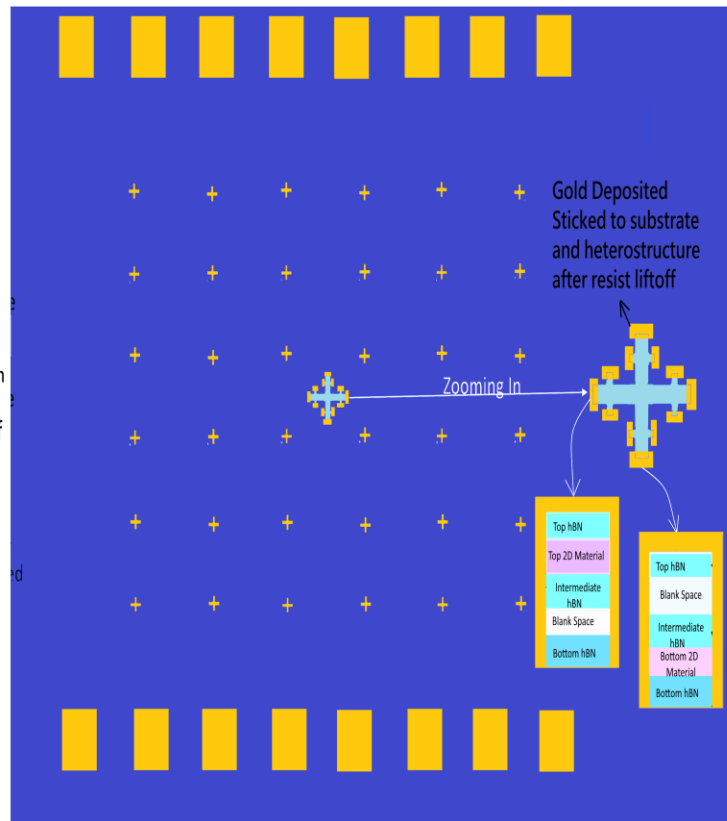
DEVICE FABRICATION



DEVICE FABRICATION (CONTINUED)

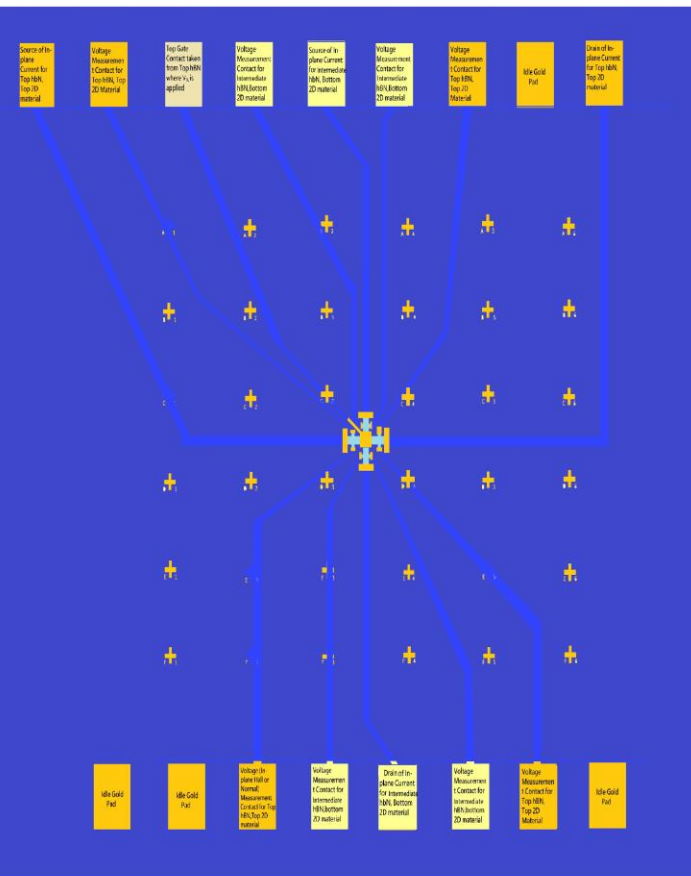


1. Gold Deposition of few hundred nanometer thickness Via Thermal Evaporator Tool ,now the gold during the deposition process enters the part of cavity in the PMMA resist in the vicinity of the van der waal heterostructure and sticks to the substrate and the heterostructure. In some cases reactive ion etching of the substrate through the cavity to get the pattern etched on the substrate may be done for better bonding of gold with the substrate and Heterostructure.
2. Now the sample is again chemically developed to remove the unexposed PMMA resist and the Gold Deposition on top of it; this step is called as resist liftoff and we get the gold deposited on the ends of the heterostructure to get gold contacts as shown in the schematic below.

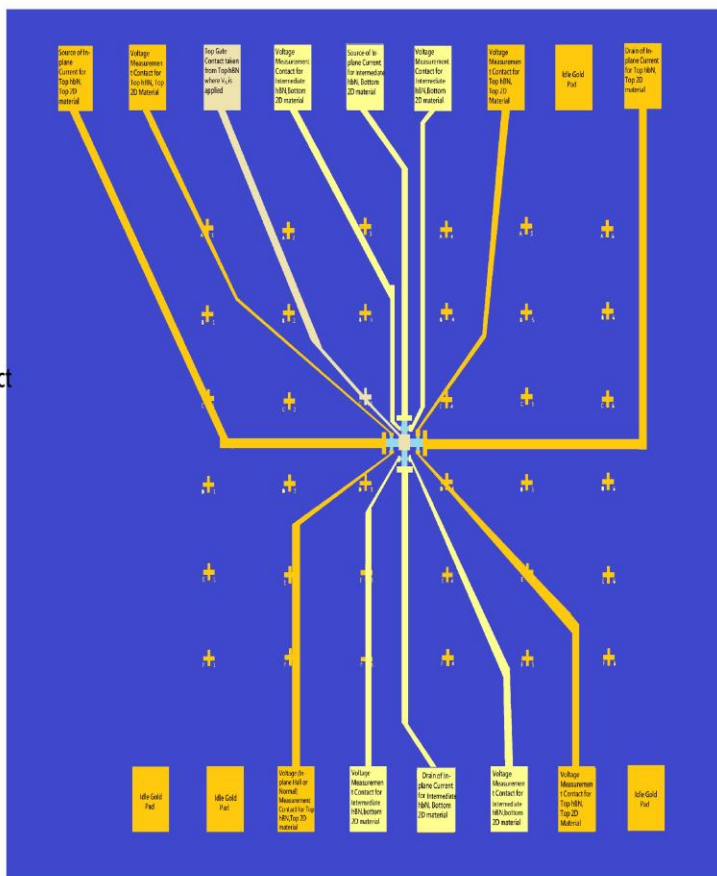


DEVICE FABRICATION (CONTINUED)

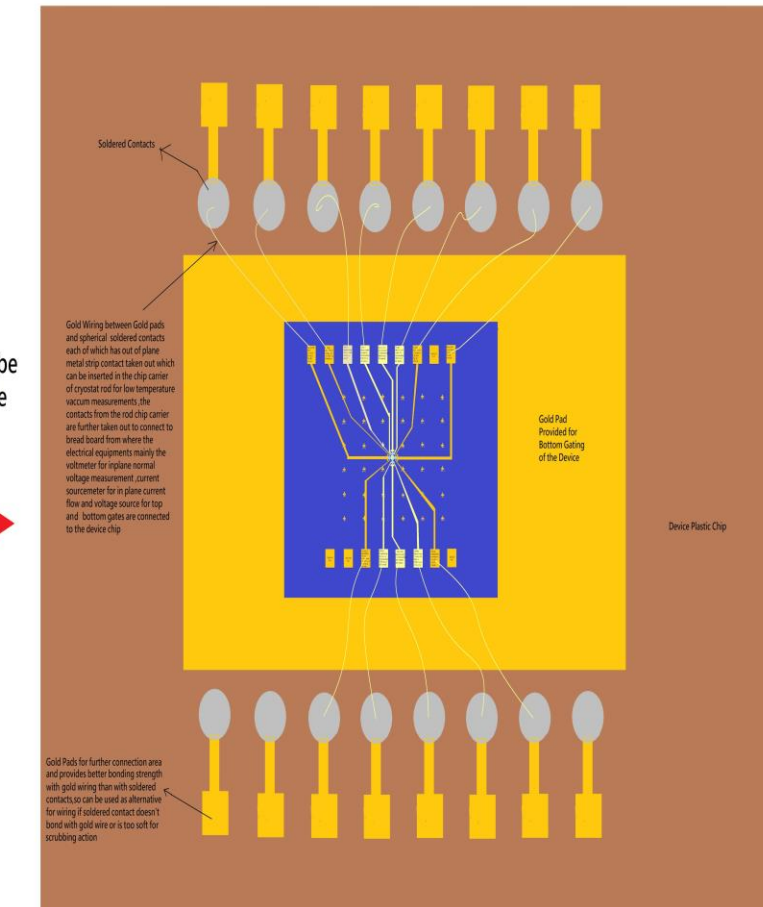
Again Perform the Same Procedure of PMMA Spin Coat, Contact Line Pattern Exposure of PMMA to electron beam, chemically develop it to remove the exposed part and create a pattern shaped cavity in PMMA as shown in figure.



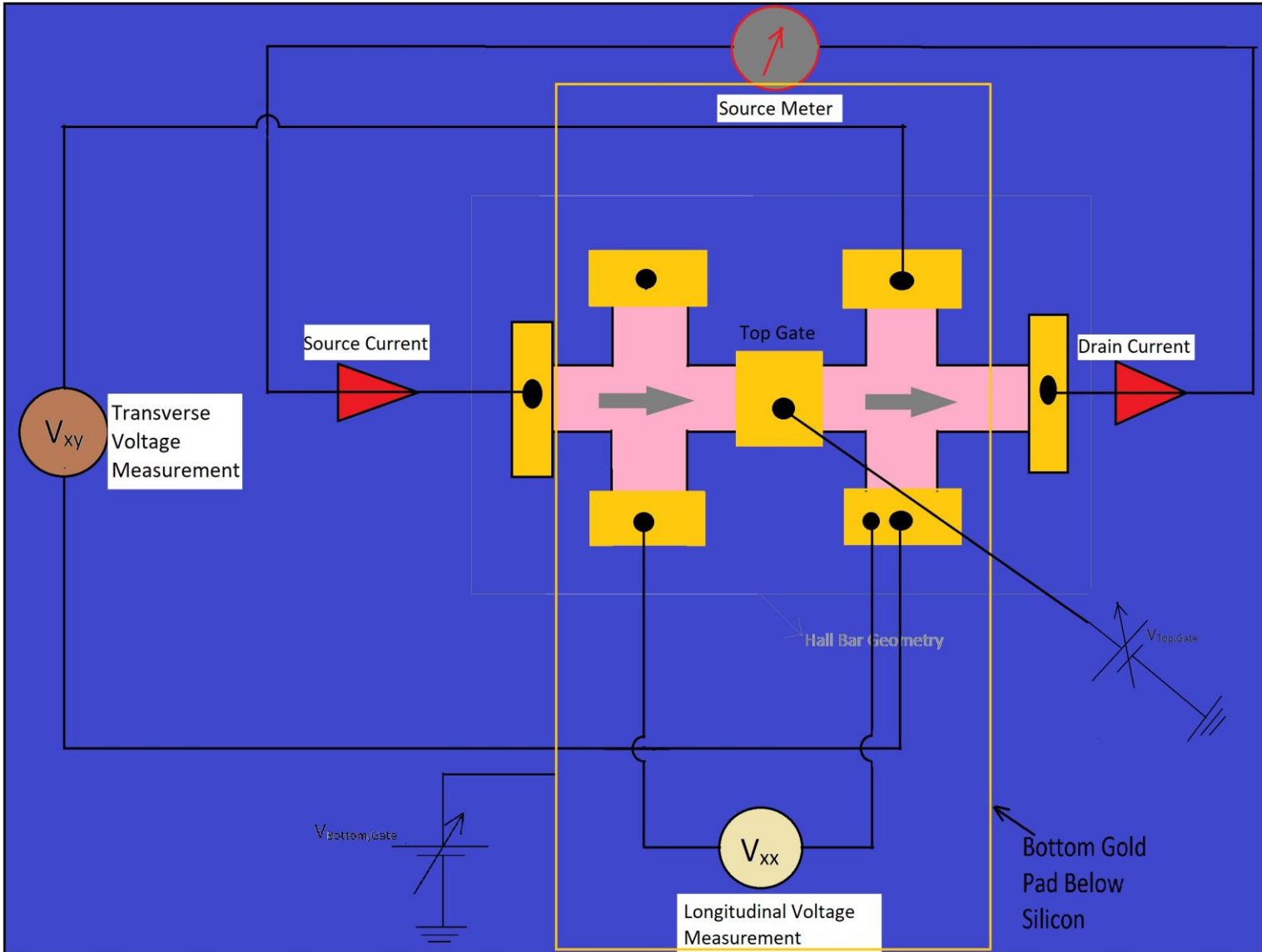
Gold Deposition
and PMMA resist
Liftoff
to get Gold Contact
Lines on the
Substrate



Device Ready to be
Gold Wired to the
Plastic Chip



MEASUREMENT SETUP (SCHEMATIC) & EXTRACTION OF CARRIER DENSITY



1. With Transverse Magnetic Field

$$R_{xx} = \frac{V_{xx}}{I_{xx}} = \frac{\rho_{xx} L}{A} = \frac{L}{\sigma_{xx} A}$$

$$V_{xy} = V_H = \frac{I_{xx} B_{zz}}{n t e}$$

$$R_H = \frac{V_H t}{I_{xx}} = - \frac{1}{n e}$$

$$\mu_H = \frac{R_H L}{R_{xx} A_{c/s}} = \frac{R_H}{R_{xx}} g = \sigma R_H$$

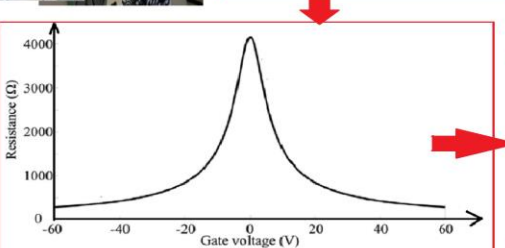
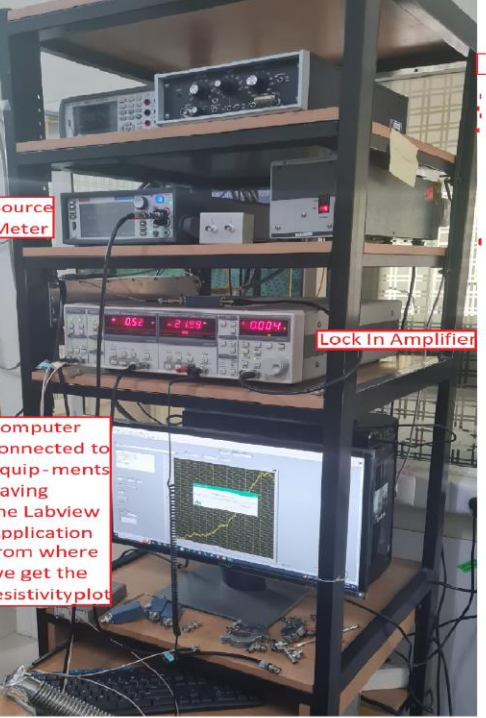
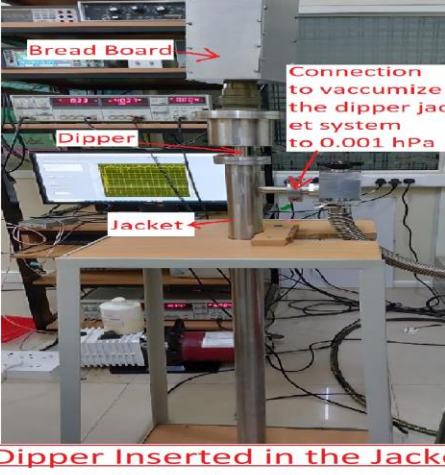
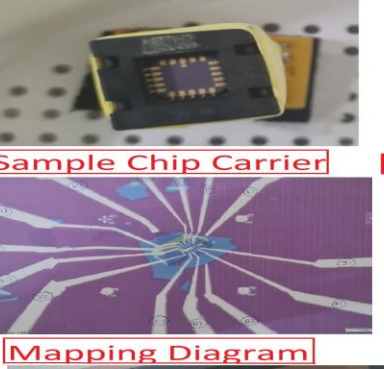
2. Without Transverse Magnetic Field

$$R_{xx} = \frac{V_{xx}}{I_{xx}} = \frac{\rho_{xx} L}{A} = \frac{L}{\sigma_{xx} A}$$

Assume Long Range Scattering,

$$\sigma_{xx} = \mu e n = \text{constant} * n$$

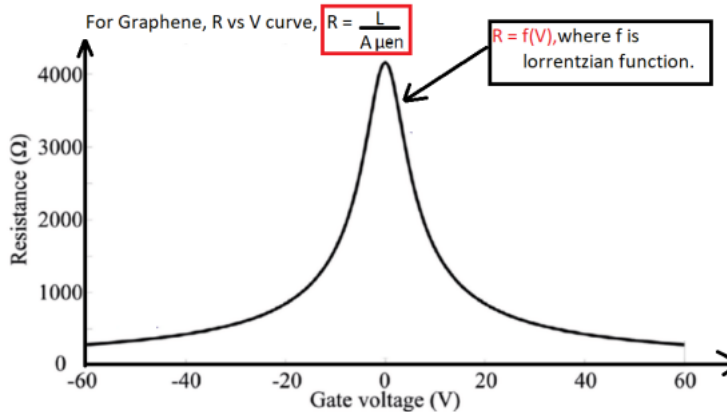
ACTUAL MEASUREMENT WORKFLOW



Extracting out the Quantum Capacitance => Curve fitting the Resistivty Plot to get the mathematical relation between the Resistance and the gate voltage and then by potential balance equation extracting the quantum capacitance

Extracting out the 15 Physical Quantities from the quantum Capacitance to completely understand the electrical transport in the 2D material and in the future realize the fascinating outlook discussed in the introduction of this thesis

QUANTUM CAPACITANCE EXTRACTED FOR GRAPHENE'S IN PLANE RESISTIVITY MEASUREMENT.



$$R = \frac{4000}{1+V^2} = \frac{L}{A_{c/s} \mu e n} \rightarrow n = \frac{L(1+V^2)}{4000 A_{c/s} \mu e}$$

Now if we consider our sample has $L_{contact} = 8 \mu m$

The Area of cross section = $8 \times 0.375 \times 10^{-15} m^2$

Assume Mobility of the carriers in graphene at low temperature = $20 m^2/Vs$ = constant as observed in most of experimental data for long range scattering (charge impurity scattering).

Actually, $\sigma_{Total} = m^* \sigma_{Ballistic\ regime\ Transport} + n^* \sigma_{Diffusive\ regime\ Transport}$

$$\sigma_{Total} = a^* \sigma_{long\ range\ or\ charged\ impurity\ scattering} + b^* \sigma_{Ballistic\ regime} + c^* \sigma_{Optical\ Phonons} + d^* \sigma_{Acoustic\ Phonons\ or\ short\ range\ scatter} + j^* \sigma_{other\ defects\ or\ reasons}$$

Now, Coming back to the calculations for graphene,

$$Therefore, n = 2.08 \times 10^{23} (1 + V^2) / m^3 \text{ volume of sample.}$$

$$n = 0.78 \times 10^{14} (1 + V^2) / m^2 \text{ overlapping area of sample}$$

$$\text{Total Number of charge carriers in the sample (N)} = n^* (\text{volume of sample})$$

$$N = 2.08 \times 10^{23} (1 + V^2) \times 8 \times 8 \times 0.375 \times 10^{-21}$$

$$N = 49.92 \times 10^2 (1 + V^2)$$

By Potential Balance,

$$V_{BG} - V_{TL} = \frac{eN}{C_{Si}} + \frac{eN}{C_{SiO_2}} + \frac{eN}{C_{BottomhBN}} + \frac{eN}{C_{Q,2D}}$$

$$V_{BG} - V_{TL} = V = \text{Gate Potential}$$

$$C_{Si} = A \epsilon_{Si} / d_{Si} = 3.7376 \text{ mF}$$

$$C_{SiO_2} = 0.832 \text{ mF}$$

$$C_{BottomhBN} = 24.064 \text{ mF}$$

Now the Potential Balance equation becomes,

$$V = 49.92 \times 10^2 (1 + V^2) e \left(\frac{1}{3.7376} + \frac{1}{0.832} + \frac{1}{24.064} + \frac{1}{C_{Q,2D}} \right)$$

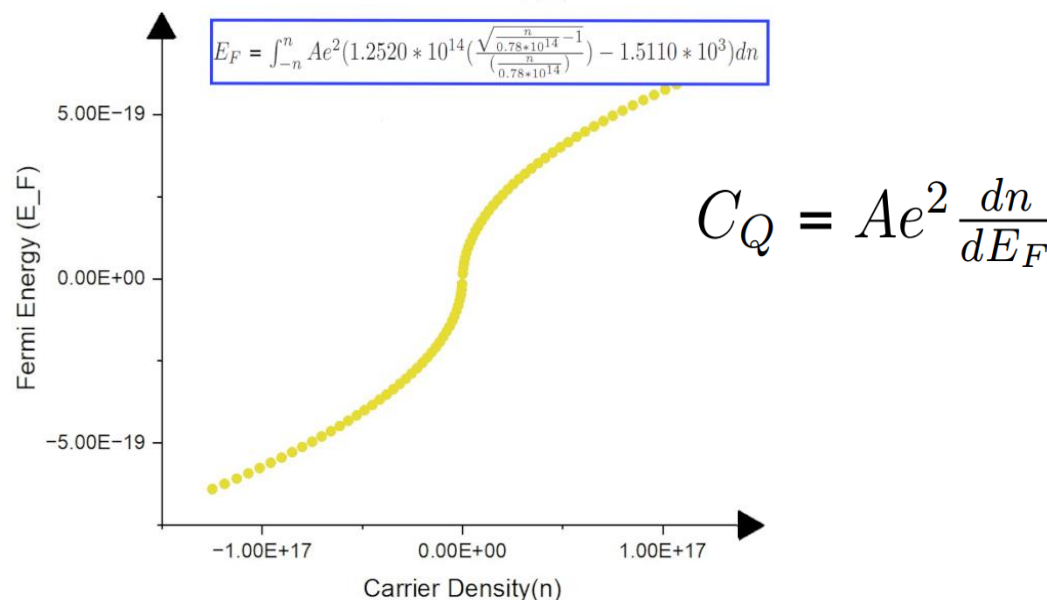
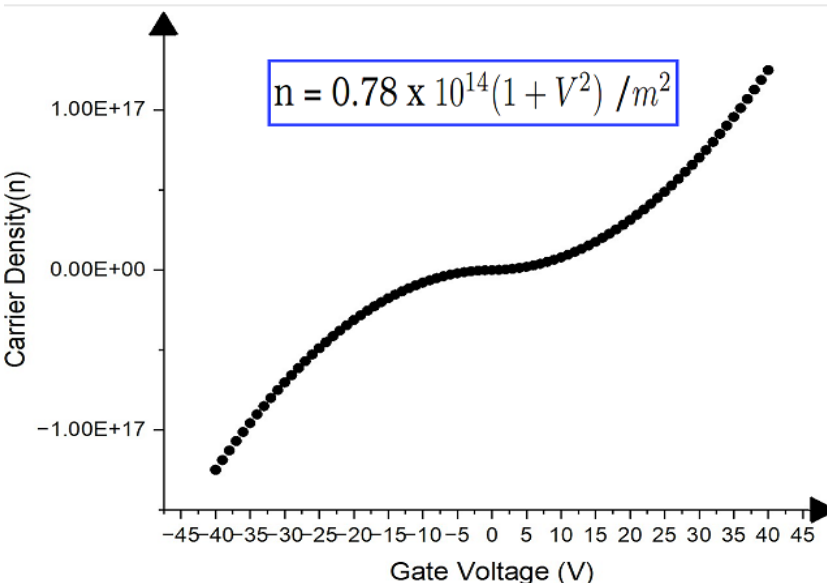
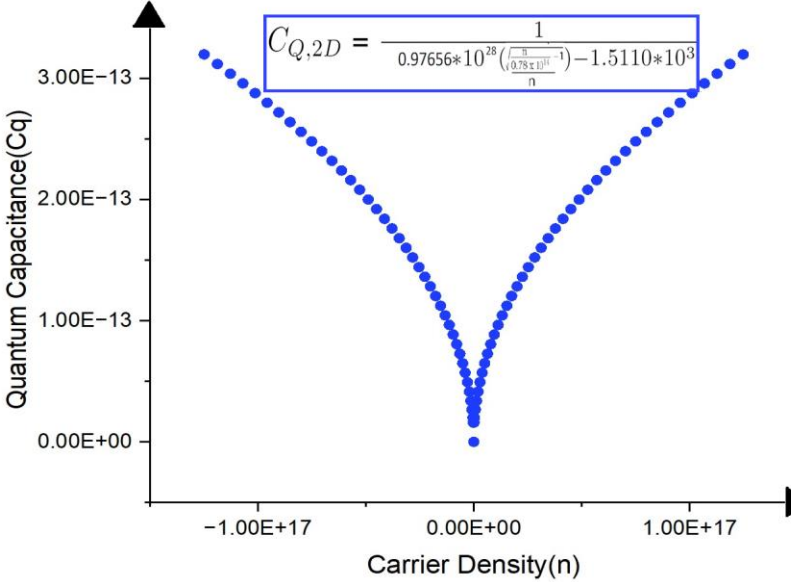
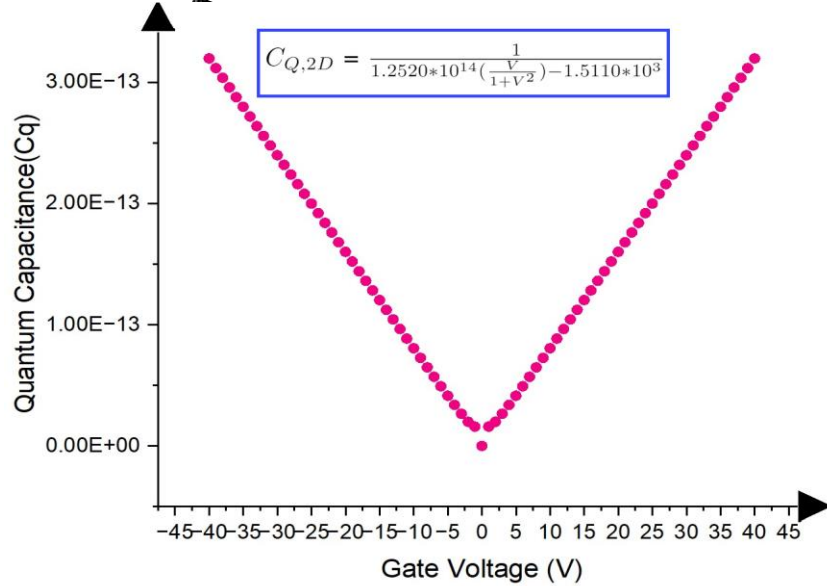
$$\frac{V}{1+V^2} = 79.872 \times 10^{-16} \left(\frac{1}{3.7376} + \frac{1}{0.832} + \frac{1}{24.064} + \frac{1}{C_{Q,2D}} \right)$$

$$\frac{V}{1+V^2} = 79.872 \times 10^{-16} \left((1.5110 \times 10^3) + \frac{1}{C_{Q,2D}} \right)$$

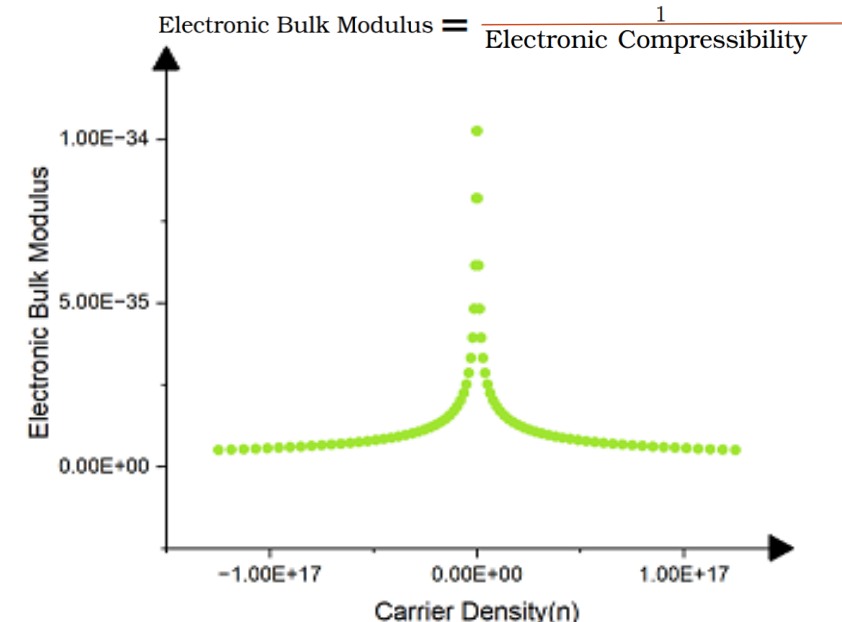
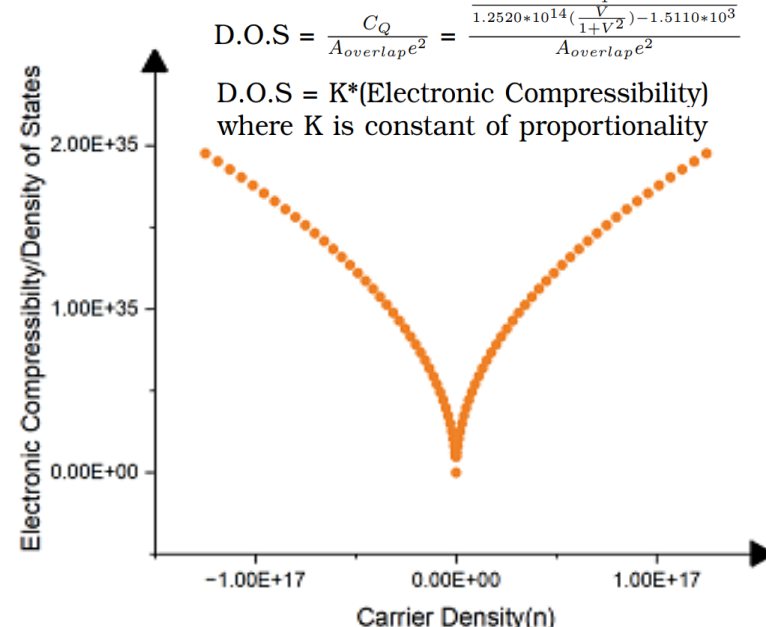
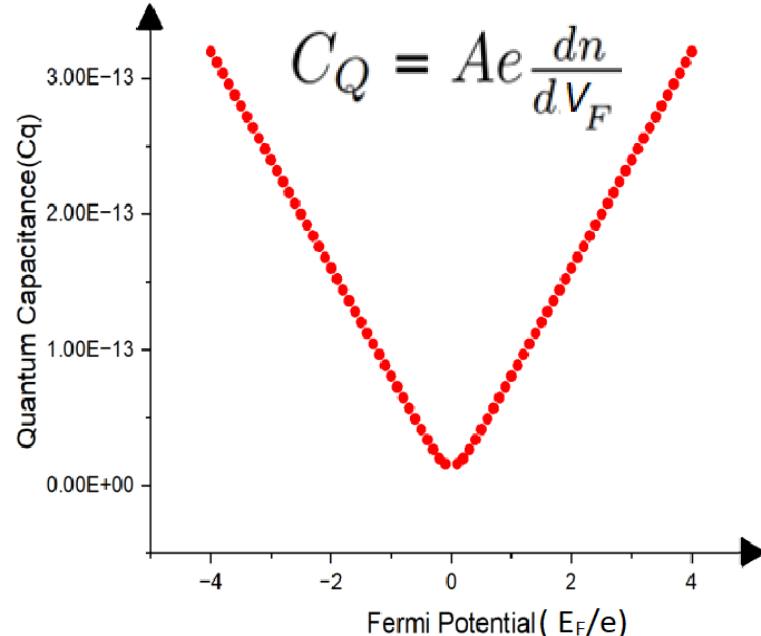
$$C_{Q,2D} = \frac{1}{1.2520 \times 10^{14} \left(\frac{V}{1+V^2} \right) - 1.5110 \times 10^3} \Rightarrow [A]$$



QUANTUM CAPACITANCE EXTRACTED FOR GRAPHENE'S IN PLANE RESISTIVITY MEASUREMENT & QUANTITIES EXTRACTED FROM QUANTUM CAPACITANCE



QUANTITIES EXTRACTED FROM QUANTUM CAPACITANCE



Now,

$$R_{\text{total}} = R_{\text{contacts}} + R_{\text{actual conductor}}$$

$$= \frac{1}{G_{\text{Ballistic conductor}}} + \frac{1-T}{G_{\text{Diffusive conductor}}}$$

$$R_{\text{total}} = (h/2e^2 M) + (h/2e^2 M)(\frac{1-T}{T}) = (\frac{h}{2e^2 M T})$$

$$R = \frac{4000}{1+V^2} = \frac{L}{A_{c/s} \mu en}$$

$$\frac{L}{A_{c/s} \mu en} = (\frac{h}{2e^2 M T}) = \text{Resistance of contacts in the ballistic regime of 2D material } * (\frac{1}{T})$$

Now we assumed that the transport is diffusive hence $\sigma = \mu en$ but this equation can be written as $\sigma = \mu e \sqrt{n} * \sqrt{n}$.

Consider a constant C that we can multiply and divide equation of R_{total} with.

Hence the resistance of contacts in the Ballistic Regime is,

$$R_{\text{contact}} = \frac{h}{2e^2 M} = \frac{L}{A_{c/s} \mu e \sqrt{n} C}$$

Define, $R_{\text{Diffusion}} = \frac{1}{T} = \frac{C}{\sqrt{n}}$ as the Diffusion Resistance fraction.

We know that Transmission function range from 0 to 1 hence C is constant introduced to satisfy this condition.

Now the maximum value of carrier density for our case is $n = 2 * 10^{17}$ for which the Resistance nears zero for graphene and hence we can safely assume $T = 1$ in that case. i.e $T = \frac{\sqrt{n}}{C}$ therefore

$$C = \sqrt{2 * 10^{17}} = 4.472 * 10^8$$

Now considering the geometric factor ($L/A_{c/s}$) to be 1 i.e neglecting the thickness of the 2D material.

$$\text{hence } M = 185.588 * 10^{-7} * \sqrt{n}$$

$$\text{and } T = 2.236 * 10^{-9} * \sqrt{n}$$

QUANTITIES EXTRACTED FROM QUANTUM CAPACITANCE

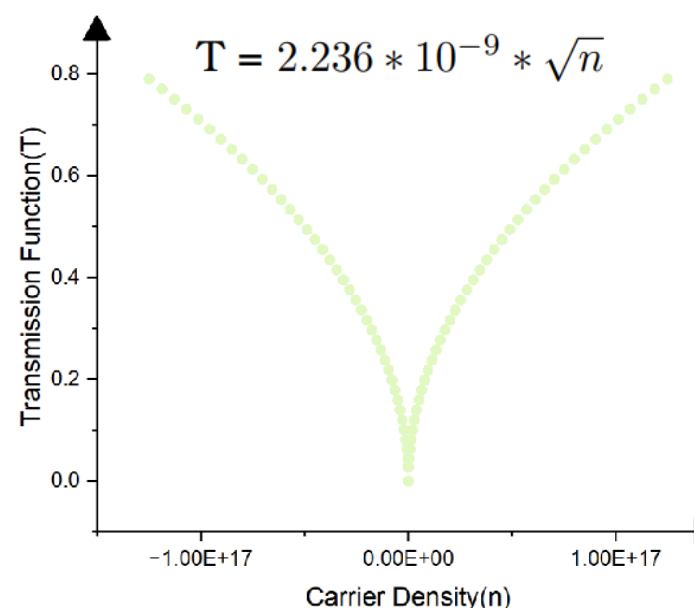
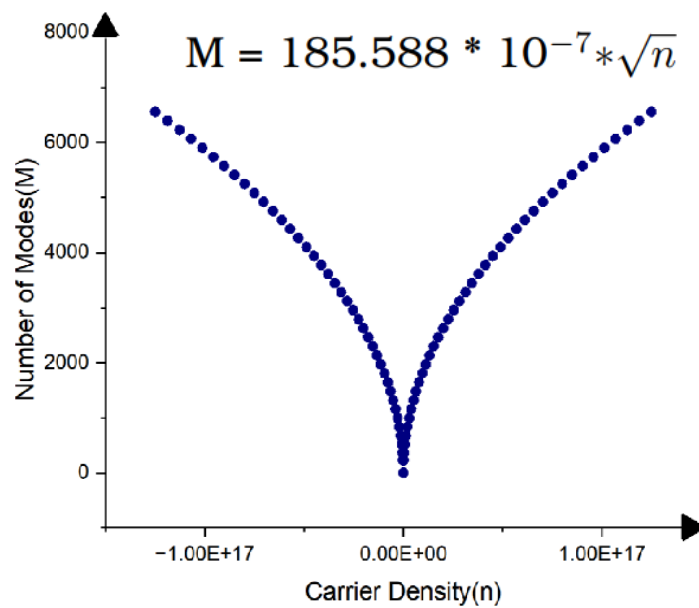
$$M = 2 * \text{Int}\left(\frac{K_F W}{\pi}\right) \text{ (Factor 2 accounts for spin degeneracy)}$$

For the sample considered $W = 8 * 10^{-6}$ m,
then K_F essentially becomes,

$$K_F = 3.6422\sqrt{n}$$

From K_F relation with n and E_F relation with n we can extract out the Fermi Velocity of the charge carriers by,

$$V_F = \frac{1}{h} \frac{dE_F}{dK_F} = \frac{2\pi}{6.64*10^{-34}} * \frac{4.48*10^{-14}(1.8229*10^{-27}n)^{0.50247}}{3.6422} = 4.9669 * 10^6 \text{ m/s}$$



$$T = \frac{2L_0}{L+L_0} = 2.236 * 10^{-9} * \sqrt{n}$$

$$\text{Hence } L_0 = \frac{0.5*L}{\frac{4.472*10^8}{\sqrt{n}} - 0.5}$$

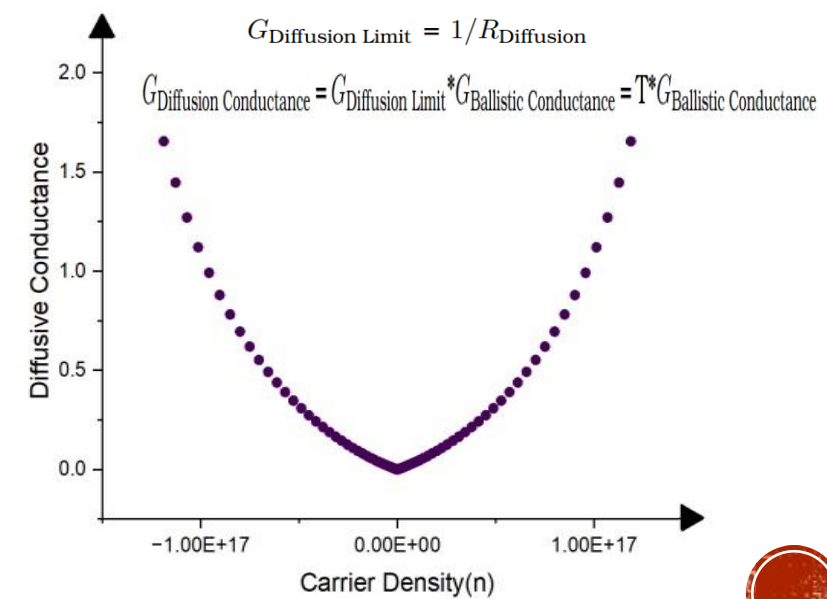
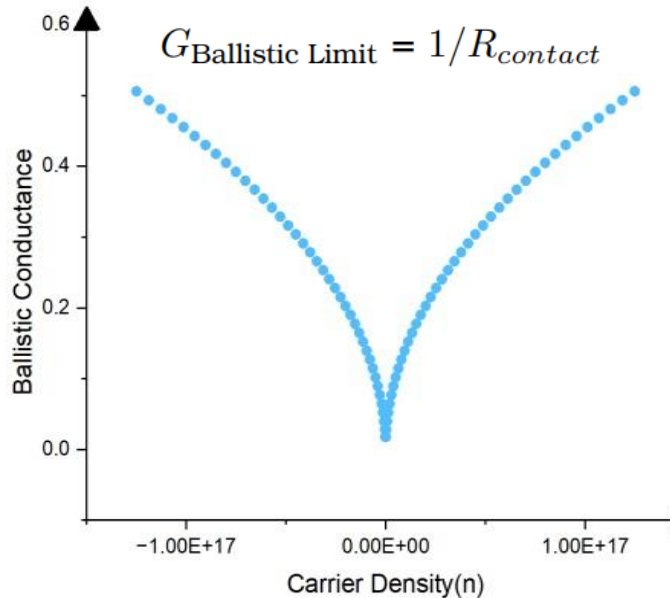
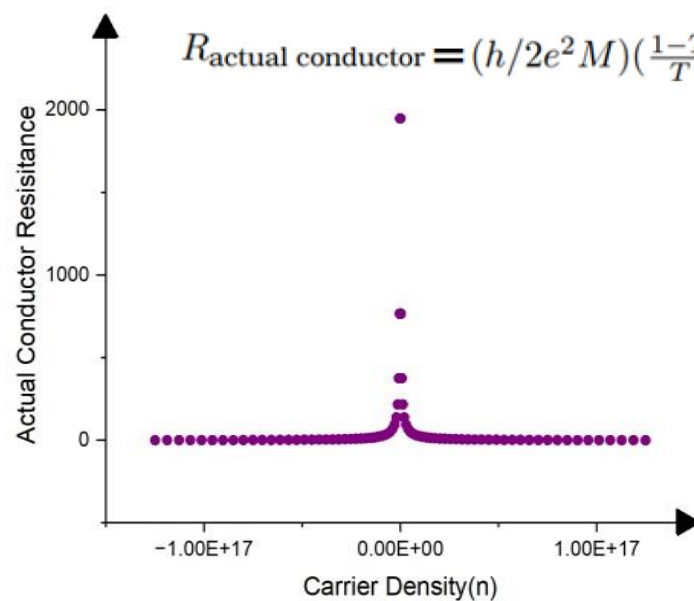
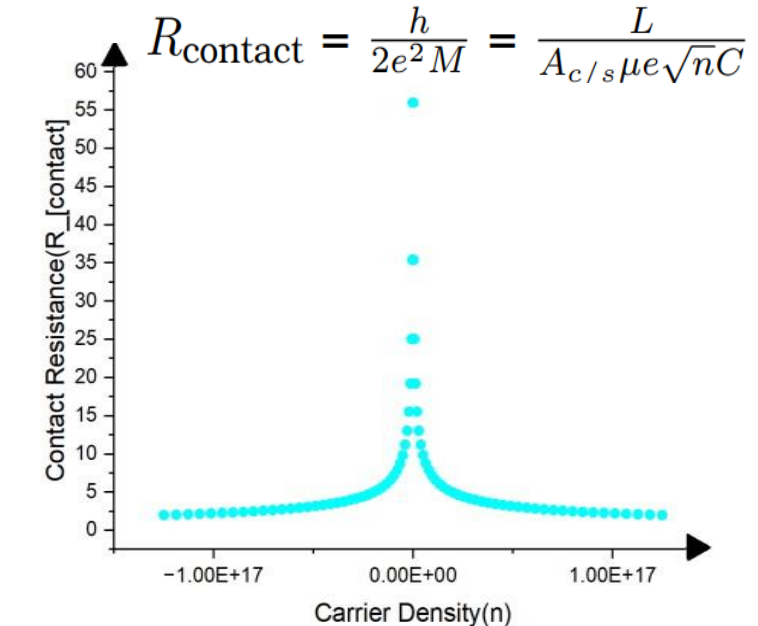
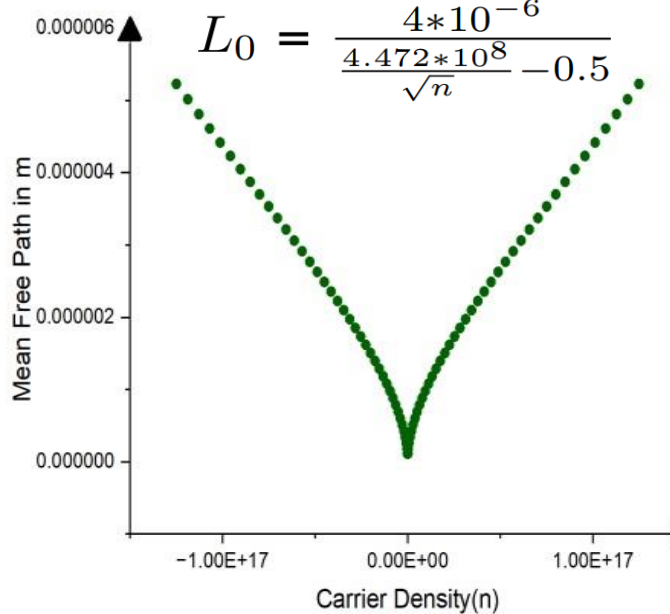
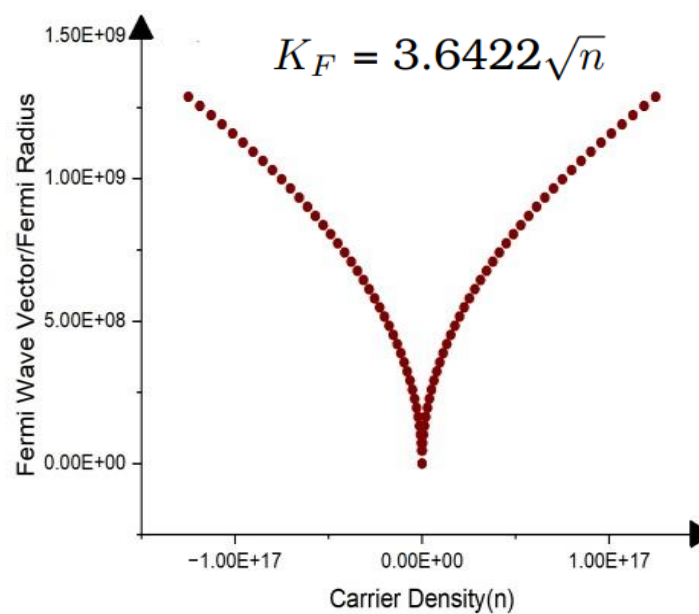
$$L_0 = \frac{0.5*L}{\frac{4.472*10^8}{\sqrt{n}} - 0.5}$$

for a Length of sample as $8 * 10^{-6}$,

$$L_0 = \frac{4*10^{-6}}{\frac{4.472*10^8}{\sqrt{n}} - 0.5}$$



QUANTITIES EXTRACTED FROM QUANTUM CAPACITANCE



FUTURE SCOPE/OUTLOOKS/IMPACTS POSSIBLE IN QUANTUM TECHNOLOGIES

From the 15 Quantities Extracted we can quantify whether the 2D material is suitable for Realizing,

1. Fault Tolerant Quantum Computer Using Ballistic Transport Regime.
2. Negative Compressibility Realizations in 2D materials.
3. Updating Theoretical Hamiltonian From Experimentally Extracted Quantum Capacitance.
4. Quantum Memory/Repeater Devices.
5. Superconductivity at Room Temperature and Room Pressure.

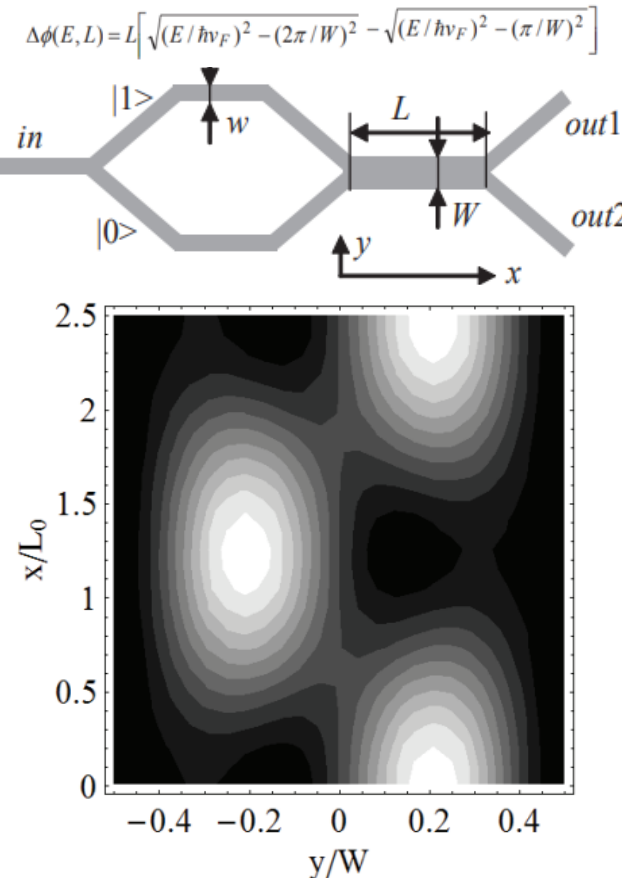
Also , Future Scope possible of this work ,

- Industrially Synthesizing the Large Sheets of Monolayers of Graphene by Lap Joint/Butt Joint.
 - Out of Plane Tunnelling Current Measurements in conducting 2D materials.
 - Mathematical Machine Learning Models for Various Phenomenons Observed In 2D materials.
- ... Possibilities with 2D materials are endless.



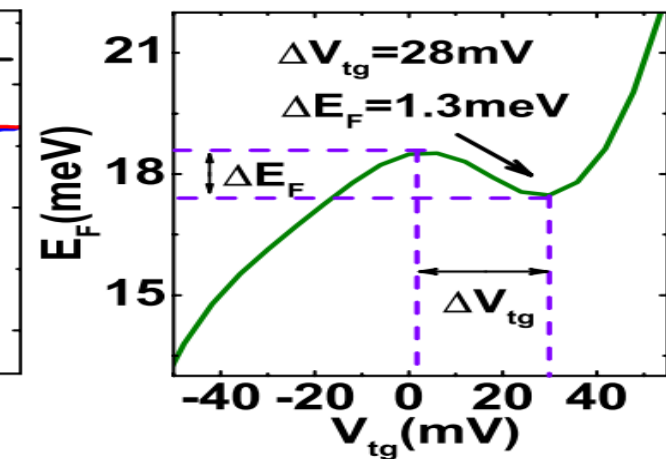
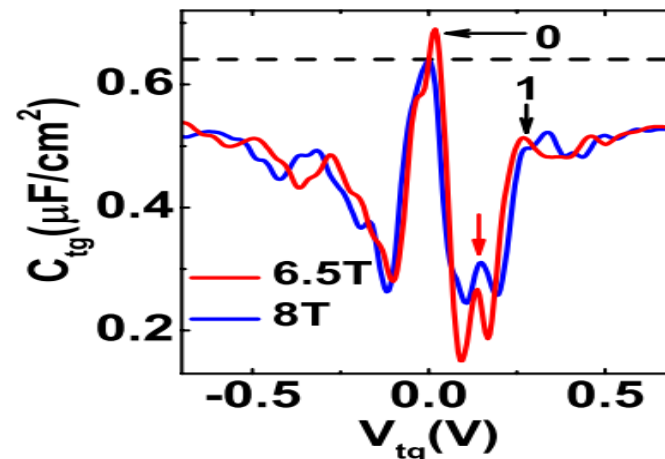
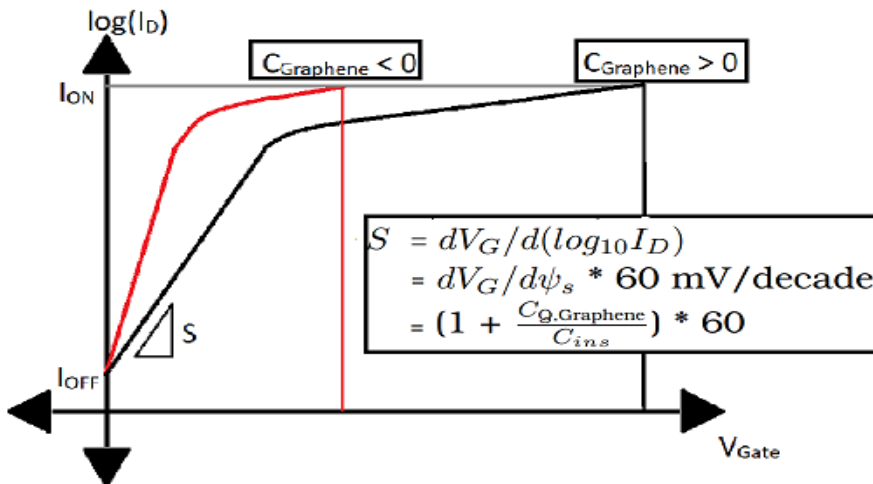
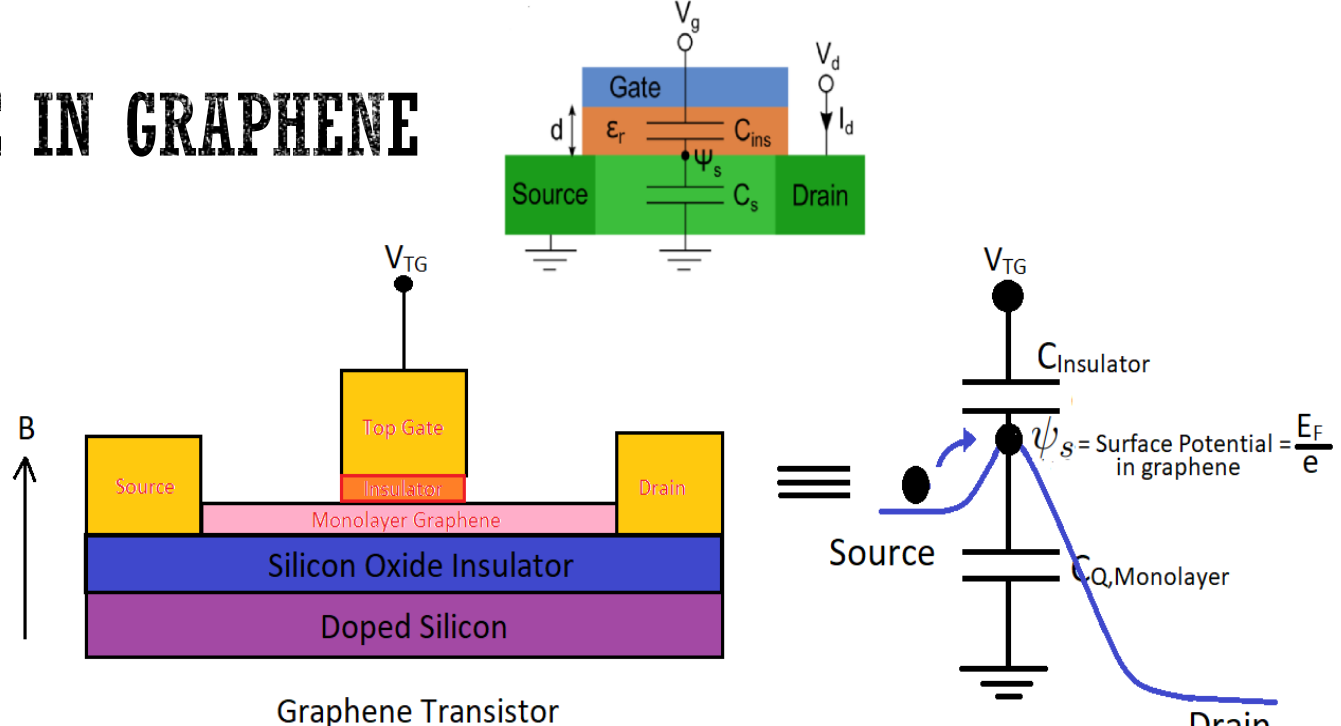
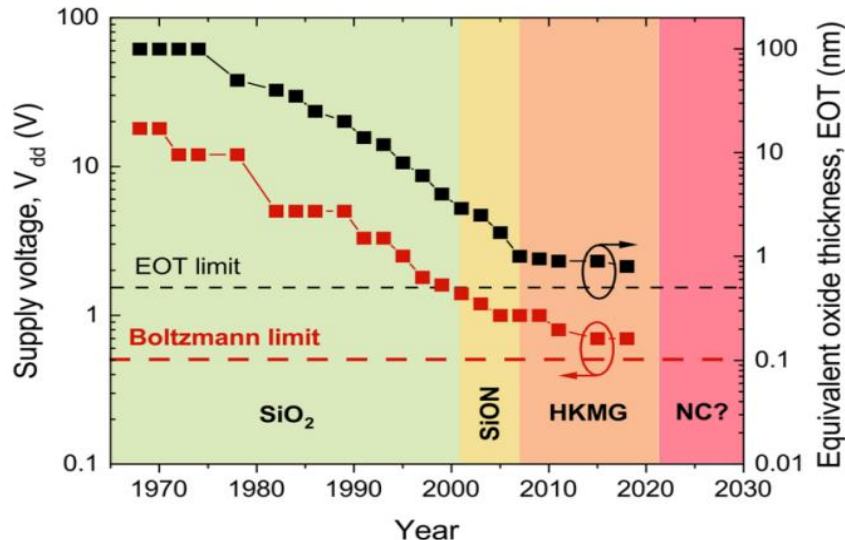
FAULT TOLERANT QUANTUM COMPUTER ROADMAP USING BALLISTIC TRANSPORT REGIME IN GRAPHENE -

- Graphene has mean free path i.e length of no scattering of electron of 10 micro-m at room temperature.
- Y channel monolayer graphene with width w allowing only propagation of one mode in one way of Y channel i.e $|0\rangle$ or $|1\rangle$, later unify it to interference bridge of width W having two modes and length L decides the amplitude of the superposition of two states of electrons via interference pattern between two propagating electron waves.



- Set of universal gates construction possible
- Quantum Circuits having maximum of 500 Quantum Gates in one mean free path of graphene is possible.
- Coming to Y direction 200000 physical qubits owing to 200 logical qubits by error correction will just be hard fabricated in 12mm width chip.
- Just Apply potential difference between input and one of the output and measure current/transmission probabilities from other output.
- After 500 Quantum gates in direction we can use quantum repeaters to reproduce the state at start of the next qubit line and start the coherence length afresh and realize required circuitry depth in x direction
- Road-Blocks – Fidelities of Circuits , Graphene has defects from fabrications which can lead to scattering and quasi-ballistic transport , Precision cutting of graphene to get graphene nano-ribbons and Fidelities of Quantum Repeaters.
- Easy to Realize and measure with already available lock in amp's and source-meter.

NEGATIVE QUANTUM CAPACITANCE IN GRAPHENE

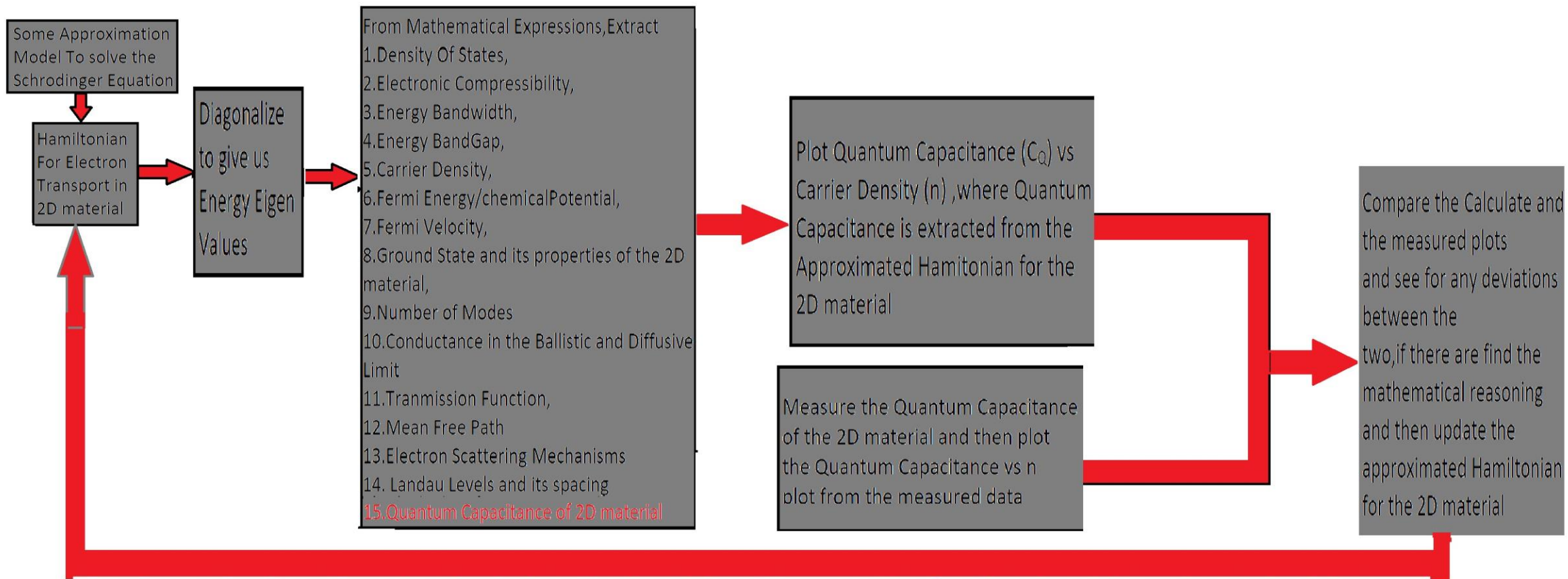


Negative compressibility observed in graphene containing resonant impurities. *Appl. Phys. Lett.* 20 May 2013; 102 (20): 203103. <https://doi.org/10.1063/1.4807394>

Michael Hoffmann, Stefan Slesazeck, and Thomas Mikolajick, "Progress and future prospects of negative capacitance electronics: A materials perspective", *APL Materials* 9, 020902 (2021)



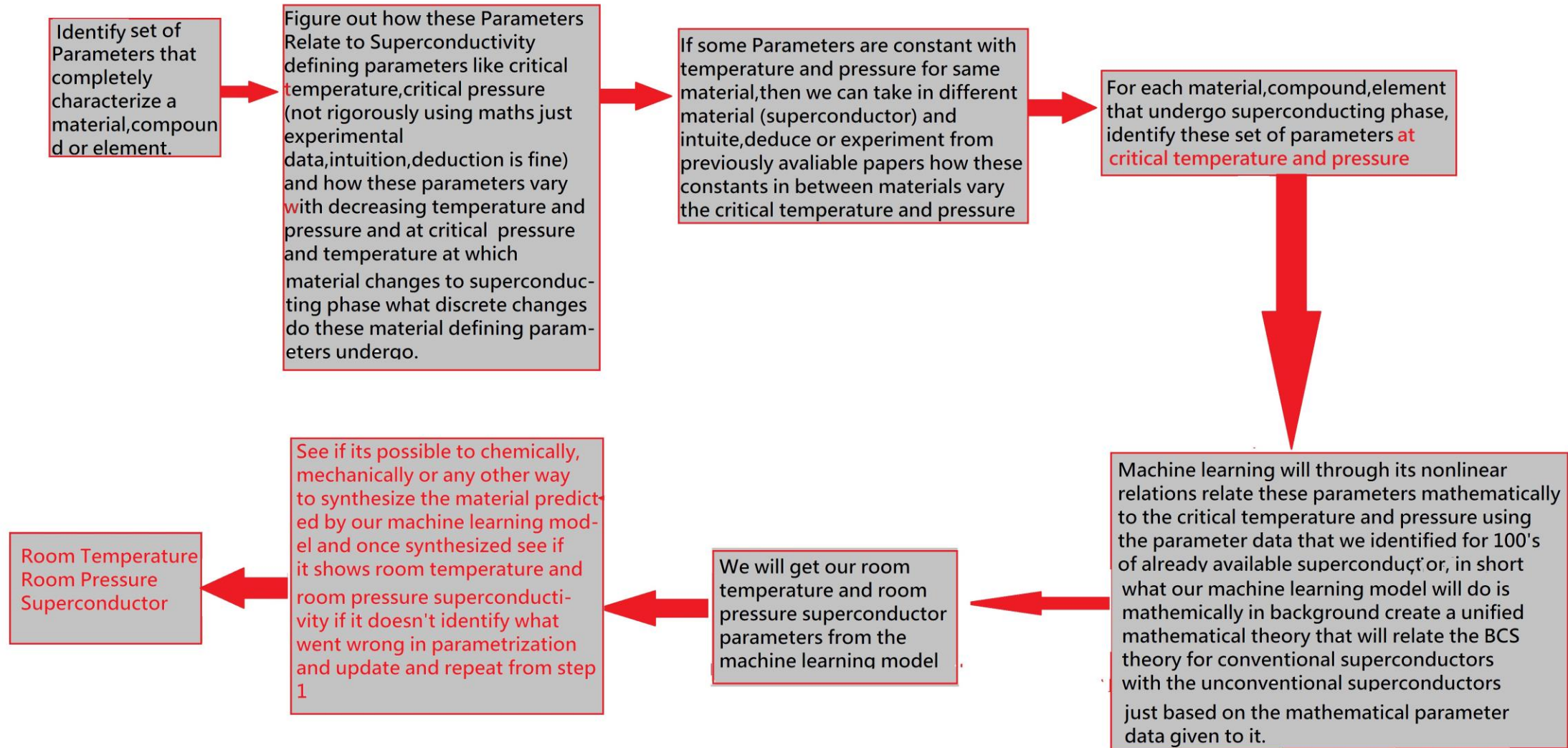
UPDATING THEORETICAL HAMILTONIAN FROM EXPERIMENTALLY EXTRACTED QUANTUM CAPACITANCE.



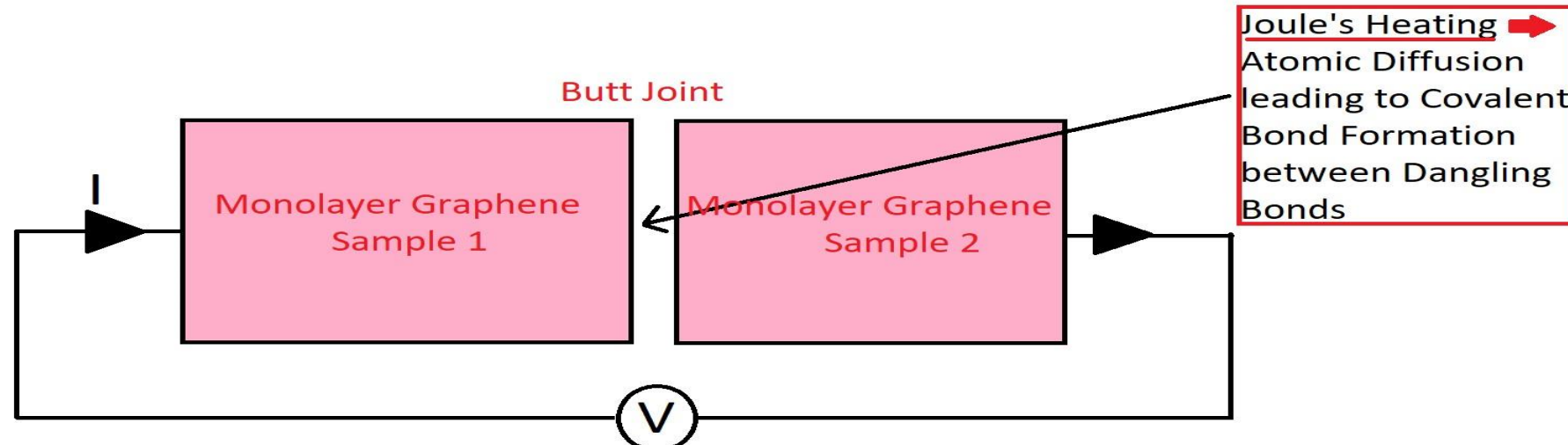
Note - Quantum Capacitance Measured can also give these 14 mathematical quantities expressed here from the mathematical expressions exactly and then we can compare those calculated values from measured data with the calculated values from approximated Hamiltonian Mathematical Expression and then update the Hamiltonian so that we can get an exact mathematical Hamiltonian and can exactly quantify it for the 2D material



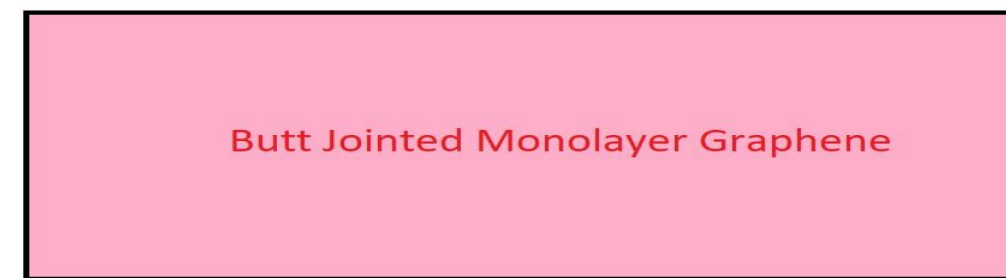
SUPER-CONDUCTIVITY AT ROOM TEMPERATURE AND PRESSURE ROAD-MAP



INDUSTRIALLY SYNTHESIZING THE LARGE SHEETS OF MONOLAYERS OF GRAPHENE BY LAP JOINT/BUTT JOINT.



Transverse Electric Field as in the case of TEM may be used to micrograph the Joint
Here the Energy source is In plane Voltage and TEM but CO₂ laser or some other energy source can also lead to similar Joule's Heating



Butt Joint with electronic and optical properties
Similar to Pristine Graphene



CONCLUSION

- Theorized a Novel Technique to Extract Quantum Capacitance which is a major improvement over the already available complex techniques of ,
 1. Constructing dielectric-2D material (whose quantum capacitance we want to measure)-dielectric-2D material (probes the top 2D material via its charge neutrality point)-dielectric using transfer technique and then carrying out in plane resistivity measurement of two Hall bar 2D material layers and ,
 2. Making hardware changes in the capacitance measurement circuit using HEMT's to reduce its parasitic capacitance.
- This novel technique of extracting quantum capacitance can be applied for any 2D material and also the expressions discussed are general and not in any way specific to graphene and hence one can extract and completely characterize the electron transport of any conducting 2D material using this technique and bring us one step closer to realizing the above mentioned fascinating outlooks

REFERENCES

- 'Electron Transport in Graphene Transistors and Heterostructures: Towards Graphene-based Nanoelectronics' thesis by Seyoung Kim (2012).
- 'Thermodynamic and Tunneling Measurements of van der Waals Heterostructures' thesis by Spencer Louis Tomarken (2019).
- D. Dragoman, "Quantum computing with graphene devices," 2016 International Semiconductor Conference (CAS), Sinaia, Romania, 2016, pp. 3-9, doi: 10.1109/SMICND.2016.7783024.
- Michael Hoffmann, Stefan Slesazeck, and Thomas Mikolajick , "Progress and future prospects of negative capacitance electronics: A materials perspective", APL Materials 9, 020902 (2021).
- Song, Jianguo Wang, Xinzhi Chang, Chang-Tang. (2014). Preparation and Characterization of Graphene Oxide. Journal of Nanomaterials. 2014. 1-6.. 10.1155/2014/276143.
- S Ramachandra Bangari.(2021) .Exploring Electronic Properties Of Twisted Bilayer Graphene,IISc ,Benguluru,India.
- Blake, P. Novoselov, K. Castro Neto, Antonio Jiang, Dingde Yang, Rongduan Booth, Timothy Geim, A. Hill, Ernie. (2007). Making graphene visible. Applied Physics Letters. 91. 10.1063/1.2768624
- Gorbachev, Roman Riaz, IbtSAM Raveendran-Nair, Rahul Jalil, Rashid Britnell, Liam Belle, B. Hill, Ernie Novoselov, K. Watanabe, K Taniguchi, Takashi Geim, A. Blake, P. (2010). Hunting for Monolayer Boron Nitride: Optical and Raman Signatures
- Blake, P. Novoselov, K. Castro Neto, Antonio Jiang, Dingde Yang, Rongduan Booth, Timothy Geim, A. Hill, Ernie. (2007). Making graphene visible. Applied Physics Letters. 91. 10.1063/1.2768624
- Gorbachev, Roman Riaz, IbtSAM Raveendran-Nair, Rahul Jalil, Rashid Britnell, Liam Belle, B. Hill, Ernie Novoselov, K. Watanabe, K Taniguchi, Takashi Geim, A. Blake, P. (2010). Hunting for Monolayer Boron Nitride: Optical and Raman Signatures
- NPTEL IIT Guwahati,"Lec 6: Raman Spectroscopy." Youtube Video, 1:18:14 . December 29,2021. <https://www.youtube.com/watch?v=6Nb04U41SkA> 10
- NPTEL-NOC IITM,"Raman Spectroscopy of Carbon Materials." Youtube Video, 35:35 . April 13,2021. <https://www.youtube.com/watch?v=6Nb04U41SkA>
- Wu, Jiangbin Lin, Miao-Ling Xin, Cong Liu, Henan Tan, Ping-Heng. (2018). Raman spectroscopy of graphene-based materials and its applications in related devices. Chemical Society Reviews. 47. 10.1039/C6CS00915H.
- Basko, D. Piscanec, S. Ferrari, A. (2009). Electron-electron interactions and doping dependence of the two-phonon Raman intensity in graphene. Physical Review B. 80. 10.1103/PhysRevB.80.165413.
- Heo, Gaeun Kim, Yong Chun, Seung-Hyun Seong, Maeng-Je. (2015). Polarized Raman spectroscopy with differing angles of laser incidence on single-layer graphene. Nanoscale Research Letters. 10. 10.1186/s11671-015-0743-4.
- Gorbachev, Roman Riaz, IbtSAM Raveendran-Nair, Rahul Jalil, Rashid Britnell, Liam Belle, B. Hill, Ernie Novoselov, K. Watanabe, K Taniguchi, Takashi Geim, A. Blake, P. (2010). Hunting for Monolayer Boron Nitride: Optical and Raman Signatures
- Xin, Cong Wu, Jiangbin Lin, Miao-Ling Xuelu, Liu Shi, Wei Venezuela, Pedro Tan, PingHeng. (2018). Anti-Stokes Raman scattering in mono- and bilayer graphenes. Nanoscale. 10. 10.1039/C8NR04554B.

REFERENCES (CONTINUED)

- Wu, Jiangbin Lin, Miao-Ling Xin, Cong Liu, Henan Tan, Ping-Heng. (2018). Raman spectroscopy of graphene-based materials and its applications in related devices. *Chemical Society Reviews*. 47. 10.1039/C6CS00915H.
- Das, A Chakraborty, Biswanath Piscanec, S. Pisana, S. Sood, A. Ferrari, A.. (2008). Phonon renormalisation in doped bilayer graphene. *Phys Rev B*. 79
- Das, A & Pisana, S. & Chakraborty, Biswanath & Piscanec, S & Saha, S & Waghmare, Umesh & Novoselov, K & Krishnamurthy, H. & Geim, A.K. & Ferrari, A.C. & Sood, A.. (2008). Monitoring dopants by Raman scattering in an electrochemically top-gated graphene transistor. *Nature nanotechnology*. 3. 210-5. 10.1038/nnano.2008.67.
- .Xin, Cong Wu, Jiangbin Lin, Miao-Ling Xuelu, Liu Shi, Wei Venezuela, Pedro Tan, PingHeng. (2018). Anti-Stokes Raman scattering in mono- and bilayer graphenes. *Nanoscale*. 10. 10.1039/C8NR04554B.
- .Wu, Jiangbin Lin, Miao-Ling Xin, Cong Liu, Henan Tan, Ping-Heng. (2018). Raman spectroscopy of graphene-based materials and its applications in related devices. *Chemical Society Reviews*. 47. 10.1039/C6CS00915H.
- Basko, D. Piscanec, S. Ferrari, A.. (2009). Electron-electron interactions and doping dependence of the two-phonon Raman intensity in graphene. *Physical Review B*. 80. 10.1103/PhysRevB.80.165413.
- Gorbachev, Roman Riaz, Ibtsem Raveendran-Nair, Rahul Jalil, Rashid Britnell, Liam Belle, B. Hill, Ernie Novoselov, K. Watanabe, K Taniguchi, Takashi Geim, A. Blake, P. (2010). Hunting for Monolayer Boron Nitride: Optical and Raman Signatures.
- Gadelha, Andreij Ohlberg, Douglas Rabelo, Cassiano Silva, Eliel Vasconcelos, Thiago Campos, Joao Luiz Lemos, Jéssica Ornelas, Vinícius Miranda, Daniel Nadas, Rafael Santana, Fabiano Watanabe, Kenji Taniguchi, Takashi Van Troeye, Benoit Lamparski, Michael Meunier, Vincent Nguyen, Viet-Hung Paszko, Dawid Charlier, Jean-Christophe Jorio, Ado. (2021). Localization of lattice dynamics in low-angle twisted bilayer graphene. *Nature*. 590. 405-409. 10.1038/s41586-021-03252-5.
- Campolina, Tiago Gadelha, Andreij Ohlberg, Douglas Watanabe, Kenji Taniguchi, Takashi Medeiros-Ribeiro, Gilberto Jorio, Ado Campos, Leonardo. (2022). Raman spectra of twisted bilayer graphene close to the magic angle.

**THANK YOU
Q&A**

